Quantized breather excitations of Fermi-Pasta-Ulam lattices

Peter S. Riseborough
Temple University, Philadelphia, Pennsylvania 19122, USA
(Received 10 October 2011; revised manuscript received 19 December 2011; published 18 January 2012)

We have calculated the lowest energy quantized breather excitations of both the β and the α Fermi-Pasta-Ulam monoatomic lattices and the diatomic β lattice within the ladder approximation. While the classical breather excitations form continua, the quantized breather excitations form a discrete hierarchy labeled by a quantum number n. Although the number of phonons is not conserved, the breather excitations correspond to multiple bound states of phonons. The $n = 2$ breather spectra are composed of resonances in the two-phonon continuum and of discrete branches of infinitely long-lived excitations. The nonlinear attributes of these excitations become more pronounced at elevated temperatures. The calculated $n = 2$ breather and the resonance of the monoatomic β lattice hybridize and exchange identity at the zone boundary and are in reasonable agreement with the results of previous calculations using the number-conserving approximation. However, by contrast, the breather spectrum of the α monoatomic lattice couples resonantly with the single-phonon spectrum and cannot be calculated within a number-conserving approximation. Furthermore, we show that for sufficiently strong nonlinearity, the α lattice breathers can be observed directly through the single-phonon inelastic neutron-scattering spectrum. As the temperature is increased, the single-phonon dispersion relation for the α lattice becomes progressively softer as the lattice instability is approached. For the diatomic β lattice, it is found that there are three distinct branches of $n = 2$ breather dispersion relations, which are associated with three distinct two-phonon continua. The two-phonon excitations form three distinct continua: One continuum corresponds to the motion of two independent acoustic phonons, another to the motion of two independent optic phonons, and the last continuum is formed by propagation of two phonons that are one of each character. Each breather dispersion relation is split off the top from of its associated continuum and remains within the forbidden gaps between the continua. The energy splittings from the top of the continua rapidly increase, and the dispersions rapidly decrease with the decreasing energy widths of the associated continua. This finding is in agreement with recent observations of sharp branches of nonlinear vibrational modes in NaI through inelastic neutron-scattering measurements. Furthermore, since the band widths of the various continua successively narrow as the magnitude of their characteristic excitation energies increase, the finding is also in agreement the theoretical prediction that breather excitations in discrete lattices should be localized in the classical limit.

DOI: 10.1103/PhysRevE.85.011129 PACS number(s): 05.90.+m, 63.20.Ry, 63.20.Pw, 63.20.dd

I. INTRODUCTION

The properties of soliton excitations have long been the subject of intensive studies dating back to the first report of their existence as shallow water waves of finite spatial extent and persistent form by Scott-Russell in 1844 [1] and the explanation of their stability by Korteweg and de Vries (KdV) in 1895 [2]. In the Korteweg and de Vries theory, the stability of the wave form is produced by the balance between the dispersion and the nonlinearity. A fuller discussion of the early history of solitons is given in Ref. [3]. The investigation of solitons received a boost in 1965 when Zabusky and Kruskal [4], while investigating the Fermi-Pasta-Ulam phenomenon, mapped it on to the KdV system. They showed numerically that when two solitons scatter, they emerge from scattering with their forms and velocities intact. Their discovery spurred an intense period of investigation in which the properties of the solutions of the KdV equation and related exactly integrable systems were found analytically using the inverse scattering method [5,6]. The use of the inverse scattering technique led to the discovery of breather excitations, which are stable oscillatory excitations of homogeneous media that have finite spatial extents and are stabilized by the nonlinear interactions. The breather excitations can be considered as being bound states of a soliton-antisolition pair in which the oscillations result from their relative state of motion. Soliton excitations not only are known to be stable in continuous systems but are also stable in discrete integrable systems [7]. Similar stable soliton-like excitations have been predicted [8–11] and observed in many physical (but nonintegrable) systems in which the discreteness of the lattice can be considered as a perturbation [12].

The properties of breather excitations are not as well known as the properties of solitons. In 1988 Sievers and Takeno hypothesized that breather excitations may also exist in discrete and higher-dimensional lattice systems [13]. Subsequently, MacKay and Aubry [14] rigorously established the existence of breather excitations in lattices that possess a local limit. In these classical systems such as the sine-Gordon system, a classical breather excitation can be considered as a bound state of a soliton and an antisoliton pair. Due to the continuous nature of the relative motion of the soliton-antisoliton pair, the classical spectrum forms a continuum. However, when the internal motion of the breathers were quantized semiclassically using the Bohr-Sommerfeld quantization procedure [15], it became evident that the breathers form a hierarchy of discrete excitations that can be considered as the bound states of multiples of small-amplitude wave excitations. An alternate method of semiclassical quantization scheme for breathers has recently been analyzed by Schulman [16], which has led to similar conclusions. The interpretation of breathers as multiphonon bound states was confirmed by the solutions of

exactly integrable quantum systems [17,18]. This realization led to investigations of the lowest members of the hierarchy of quantized breathers in nonintegrable lattices by means of standard many-body methods [19–21]. Extensive reviews of the properties of classical and quantum breathers are given in Refs. [22–24]. The existence and stability of quantum breathers in models [25] such as the discrete nonlinear Schrödinger equation [26], the ϕ^4 lattice [27,28], and related systems [29] are well established. However, the existence of quantum breathers in the Fermi-Pasta-Ulam lattice [30] has not been proved since the interaction in the Fermi-Pasta-Ulam model is nonlocal and is not of the type considered by MacKay and Aubry [14] (although breather excitations have been shown to exist in the classical Fermi-Pasta-Ulam model by Flach and Gorbach [31]). Furthermore, as the anharmonic interaction in the Fermi-Pasta-Ulam model does not preserve the number of elementary excitations, the results found [32–34] by truncating the Hamiltonian to only include number-conserving processes [35] should not be considered conclusive unless confirmed by other methods.

Breather excitations have recently been reported [36] to exist in the high-temperature regime of the three-dimensional ionic crystal NaI. Instead of the continuous excitation spectrum expected for classical breathers, the observed spectrum consisted of a sharp discrete peak. This observation indicates that the breather excitations ought to be described in the quantum limit where quantization of the internal oscillatory degrees of freedom is expected to result in a hierarchy of discrete excitations. Furthermore, the momentum dependence of the scattering cross section indicates that the breathers show up in the single-phonon contribution instead of the continua of multiphonon excitations [37–39]. In a previous paper [40], we have investigated $n = 2$ quantized breathers of the β lattice using another method, valid at low temperatures. The method is based on the realization that the ground state has the form of a linear superposition of states containing even numbers of phonons. An approximate $n = 2$ excited state is obtained from the ground state by the action of an operator with a two-phonon creation and two-phonon annihilation component. Inspection of the spatial dependence of the various components of the $n = 2$ excitation operator revealed the localized nature of the excitation [40]. Proville has addressed the spatial and temporal correspondence between the classical and quantum breathers of the nonlinear Klein-Gordon lattice [41], by forming a Wannier wave packet as a linear superposition of energy eigenstates that exhibited both the localized and oscillatory nature of the quantum excitations. In this paper, we shall investigate the lowest members of the hierarchy of quantized breathers in the α and β Fermi-Pasta-Ulam problem within the ladder approximation. Unlike our previous method, the present method should be valid at finite temperatures. For the β lattice we shall neglect the single-phonon self-energy; however, the inclusion of the single-phonon self-energy will turn out to be crucial for the α lattice. We find that the cubic anharmonic interaction of the α lattice couples the spectrum of single-phonon excitations to the continuum of two-phonon excitations in accordance with both the earlier theoretical results of Leath and Watson [42] and the experimental results of Manley *et al.* [36].

A diatomic lattice is expected to have a much richer lattice vibration spectrum than a lattice with a monoatomic basis. The existence of breathers for the classical diatomic Fermi-Pasta-Ulam lattice were first predicted by Livi *et al.* [43] in the limit of vanishingly small mass ratios and were more thoroughly investigated by Maniadis [44] and by James and Noble [45] for arbitrary mass ratios. Recently Yoshimura [46] has provided an alternate formulation of the proof of existence and stability of the breathers. The breather excitations consist of "optic breathers," which have frequencies above the optic phonons, and as "acoustic breathers," which have frequencies that lie within the gap between the acoustic and the optic phonons. Therefore, in this paper, we shall also investigate the dispersion relations for the $n = 1$ and 2 breather excitations of the quantal diatomic Fermi-Pasta-Ulam lattice.

The manuscript is structured as follows: In Sec. II we describe the Hamiltonian for the β Fermi-Pasta-Ulam lattice, and in Sec. III we shall present the calculation of the two-phonon propagators for the η lattice. In Sec. IV we shall display the hamiltonian of the α lattice and calculate its two-phonon propagator. In Sec. V the results for the monoatomic lattices will be discussed. The diatomic Fermi-Pasta-Ulam lattice will be introduced in Sec. VI; the ladder approximation will be discussed in Sec. VII; the components of the two-phon propagator will be discussed in Sec. VIII; and the results will be presented in Sec. IX. The conclusions will be presented in Sec. X.

II. THE β FERMI-PASTA-ULAM HAMILTONIAN

The Hamiltonian for the discrete quartic Fermi-Pasta-Ulam chain can be written as

$$\hat{H} = \sum_i \left[\frac{\hat{P}_i^2}{2M} + \frac{M\omega_0^2}{2}(\hat{u}_i - \hat{u}_{i+1})^2 \right] + \frac{K_4}{12} \sum_i (\hat{u}_i - \hat{u}_{i+1})^4 \tag{1}$$

in which $\hat{u}_i$ is the operator for the atom at the ith lattice site, which represents its displacement from its equilibrium position, and $\hat{P}_i$ is the momentum operator for the same atom. The first two terms in the Hamiltonian represent the approximate harmonic Hamiltonian, and the third term, proportional to K_4, represents the anharmonic interaction. It should be noted that the Hamiltonian is invariant under the continuous transformation $u_i \to u_i + \delta$. The assumed spontaneously broken symmetry of the ground state is responsible for the occurrence of Goldstone modes.

The spatial Fourier transforms of the coordinates and momenta operators of the atoms are defined as

$$\begin{aligned} \hat{u}_q &= \frac{1}{\sqrt{N}} \sum_i \exp[iqR_i]\hat{u}_i, \\ \hat{P}_q &= \frac{1}{\sqrt{N}} \sum_i \exp[iqR_i]\hat{P}_i, \end{aligned} \tag{2}$$

where R_i represents the mean equilibrium position of the ith atom. The Hamiltonian can be rewritten in terms of operators

in the harmonic normal mode basis as

$$\hat{H} = \sum_q \left[\frac{\hat{P}_q \hat{P}_q^\dagger}{2M} + M\omega_0^2(1-\cos q)\hat{u}_q \hat{u}_q^\dagger \right] + \frac{K_4}{12N} \sum_{k_1,k_2,k_3,k_4} \Delta_{k_1+k_2+k_3+k_4} \prod_{j=1}^{4} \times \left\{ 2\sin\frac{k_j}{2} \exp\left[-i\frac{k_j}{2} \right] \hat{u}_{k_j} \right\}. \quad (3)$$

Since the anharmonic interaction has a separable form, the ladder approximation for the two-particle excitations can be solved exactly.

The harmonic part of the Hamiltonian can be second quantized and diagonalized by the substitutions

$$\hat{P}_q = i\left(\frac{M\hbar\omega_q}{2} \right)^{\frac{1}{2}} (a_{-q}^\dagger - a_q), \qquad \hat{u}_q = \left(\frac{\hbar}{2M\omega_q} \right)^{\frac{1}{2}} (a_q^\dagger + a_{-q}), \quad (4)$$

where, respectively, $a_q^\dagger$ and a_q are the boson creation and annihilation operators and where the phonon dispersion relation is given by

$$\omega_q^2 = 2\omega_0^2(1-\cos q) = 4\omega_0^2 \sin^2\frac{q}{2}. \quad (5)$$

Thus, the Hamiltonian of the β Fermi-Pasta-Ulam lattice has the second quantized form

$$\hat{H} = \sum_q \frac{\hbar\omega_q}{2}(a_q^\dagger a_q + a_q a_q^\dagger) + \hat{H}_{\rm int}, \quad (6)$$

where the interaction Hamiltonian has the form

$$\hat{H}_{\rm int} = \left(\frac{I_4}{12N} \right) \sum_{k_1,k_2,k_3,k_4} \Delta_{k_1+k_2+k_3+k_4} \prod_{j=1}^{4} \left\{ F_{k_j}(a_{k_j}^\dagger + a_{-k_j}) \right\}, \quad (7)$$

where the repulsive interaction strength I_4 (with units of energy) is defined as

$$I_4 = \left(\frac{\hbar^2 K_4}{M^2\omega_0^2} \right), \quad (8)$$

and where the complex form factors F_q are given by

$$F_q = \left(\frac{\sin\frac{q}{2} \exp\left[-i\frac{q}{2} \right]}{\sqrt{|\sin\frac{q}{2}|}} \right). \quad (9)$$

III. THE β-LATTICE TWO-PHONON PROPAGATORS

The two-phonon propagator has the form of a four by four matrix $D_{q,k,k'}^{(\alpha),(\beta)}(t)$, which involves the expectation value of the product of two two-phonon operators $\hat{A}_{q,k}^{(\alpha)}(t)$, one evaluated at time t and the other at time zero. The components of the two-phonon propagator are expressed as

$$D_{q,k,k'}^{(\alpha),(\beta)}(t) = -\frac{i}{\hbar}\langle \hat{T}\, \hat{A}_{q,k}^{(\alpha)}(t) \hat{A}_{q,k'}^{(\beta)\,\dagger}(0) \rangle, \quad (10)$$

where $\hat{T}$ is Wick's time-ordering operator. The two-phonon operators are defined as

$$\hat{A}_{q,k}^{(++)} \equiv a_{\frac{q}{2}+k}^\dagger a_{\frac{q}{2}-k}^\dagger, \quad \hat{A}_{q,k}^{(+-)} \equiv a_{\frac{q}{2}+k}^\dagger a_{-\frac{q}{2}+k}, \quad \hat{A}_{q,k}^{(-+)} \equiv a_{-\frac{q}{2}-k} a_{\frac{q}{2}-k}^\dagger, \quad \hat{A}_{q,k}^{(--)} \equiv a_{-\frac{q}{2}-k} a_{-\frac{q}{2}+k}, \quad (11)$$

where the pair of indices (ab), in which a and b are taken from the set $\{+,-\}$, are denoted by a single index (α) that takes on four values. It should be noted that, due to the bosonic character of the creation and annihilation operators, the propagator with index (ab) and momentum k is identical to the propagator with indices (ba) and momentum $-k$. Hence, to avoid ambiguity, the value of k is restricted to be positive. The components of the propagator are to be evaluated from the equations of motion

$$i\hbar\frac{\partial}{\partial t} D_{q,k,k'}^{(\alpha),(\beta)}(t) = \delta(t)\langle \left[\hat{A}_{q,k}^{(\alpha)}(0), \hat{A}_{q,k'}^{(\beta)\,\dagger}(0) \right] \rangle - \frac{i}{\hbar}\langle \hat{T}\left[\hat{A}_{q,k}^{(\alpha)}(t), \hat{H}_0(t) \right] \hat{A}_{q,k'}^{(\beta)\,\dagger}(0) \rangle - \frac{i}{\hbar}\langle \hat{T}\left[\hat{A}_{q,k}^{(\alpha)}(t), \hat{H}_{\rm int}(t) \right] \hat{A}_{q,k'}^{(\beta)\,\dagger}(0) \rangle, \quad (12)$$

which involve equal time commutators. The equations of motion are to be truncated according to the ladder approximation, depicted diagramatically in Fig. 1, in which the nontrivial single-phonon self-energies are neglected. After representing the interaction as a product of four identical factors as in Eq. (7), the expectation value involving the commutator

$$\left[\hat{A}_{q,k}^{\alpha}, \hat{H}_{\rm int} \right] \quad (13)$$

in the last term of Eq. (12) can be approximated by setting

$$\left[\hat{A}_{q,k}^{(\alpha)}, \hat{u}_{k_1}\hat{u}_{k_2}\hat{u}_{k_3}\hat{u}_{k_4} \right] \approx 6\langle \left[\hat{A}_{q,k}^{(\alpha)}, \hat{u}_{k_1}\hat{u}_{k_2} \right] \rangle \hat{u}_{k_3}\hat{u}_{k_4} + 6\left[\hat{A}_{q,k}^{(\alpha)}, \hat{u}_{k_1}\hat{u}_{k_2} \right] \langle \hat{u}_{k_3}\hat{u}_{k_4} \rangle. \quad (14)$$

In the above expression, the factor of 6 comes from the invariance of the commutator in expression (13) under permutation of the summation indices k_j. The last term in Eq. (14) represents a frequency-independent contribution to the phonon self-energy, which can be absorbed as the lowest-order temperature-dependent renormalization of the harmonic phonon frequencies [47]

$$\omega_q \approx 2\omega_0 \left| \sin\frac{q}{2} \right| \left[1 + \left(\frac{I_4}{2N\hbar\omega_0} \right) \sum_{k_1} \left| \sin\frac{k_1}{2} \right| (1+2N_{k_1}) \right], \quad (15)$$

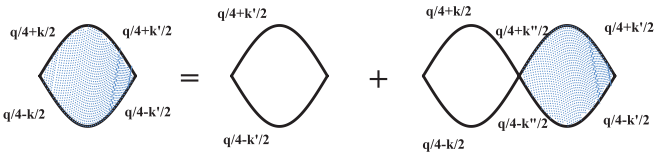

FIG. 1. (Color online) The Ladder Approximation to the two-particle Dyson equation for the β Fermi-Pasta-Ulam lattice. The interacting two-particle propagators are denoted by the shaded bubbles, and the noninteracting two-particle propagators are denoted by open bubbles. The interaction I_4 is represented by the vertex connecting two bubbles.

where the summation over k_1 runs over both positive and negative values of k. The anomalous one-phonon propagators are also eliminated if one substitutes this renormalization into Eqs. (4). This shift will not be considered any further. After truncation of the equations of motion, it is seen that the components of the two-phonon propagators satisfy a closed set of inhomogeneous first-order linear differential equations.

On Fourier transforming the set of differential equations where the Fourier transformed propagator components $D^{(\alpha),(\beta)}_{q,k,k'}(\omega)$ are defined via

$$D^{(\alpha),(\beta)}_{q,k,k'}(\omega) = \int_{-\infty}^{\infty} dt \exp[-i\omega t] D^{(\alpha),(\beta)}_{q,k,k'}(t), \tag{16}$$

one finds that the differential equations reduce to a set of coupled algebraic equations. The components of the unperturbed two-phonon propagators are diagonal in the indices α and β and in the crystal momenta k and k'. The nonzero parts of the noninteracting propagator are denoted by $D^{(\alpha),(0)}_{q,k,k}(\omega)$. The components of the unperturbed two-phonon propagators are evaluated as

$$D^{(\pm\mp),(0)}_{q,k,k}(\omega) = -\frac{\mp\left[\frac{1}{2} + N_{\frac{q}{2}+k}\right] \pm \left[\frac{1}{2} + N_{\frac{q}{2}-k}\right]}{\hbar\left(-\omega \pm \omega_{\frac{q}{2}+k} \mp \omega_{\frac{q}{2}-k}\right)}, \tag{17}$$

where the $\pm$ and $\mp$ signs are to be chosen independently. When expressed in terms of the noninteracting propagators, the closed set of algebraic equations take the form

$$D^{(\alpha),(\beta)}_{q,k,k'}(\omega) = D^{(\alpha),(0)}_{q,k,k}(\omega)\delta^{(\alpha),(\beta)}\Delta_{k-k'} + D^{(\alpha),(0)}_{q,k,k}(\omega) F^*_{\frac{q}{2}+k} F^*_{\frac{q}{2}-k} \times \frac{2I_4}{N} \sum_{\gamma,k''} F_{\frac{q}{2}+k''} F_{\frac{q}{2}-k''} D^{(\gamma),(\beta)}_{q,k'',k'}(\omega). \tag{18}$$

It is seen that the phase factors originating from the interaction term cancel. On multiplying the above equation for $D^{(\alpha),(\beta)}_{q,k,k'}(\omega)$ by the factor

$$F_{\frac{q}{2}+k} F_{\frac{q}{2}-k}, \tag{19}$$

and summing over k, one finds

$$\sum_{\alpha,k} F_{\frac{q}{2}+k} F_{\frac{q}{2}-k} D^{(\alpha),(\beta)}_{q,k,k'}(\omega) = \frac{F_{\frac{q}{2}+k'} F_{\frac{q}{2}-k'} D^{(\beta),(0)}_{q,k',k'}(\omega)}{1 - I_4 \sum_\gamma \Pi^{(\gamma)}_q(\omega)}, \tag{20}$$

where the functions $\Pi^{(\gamma)}_q(\omega)$ have been defined as

$$\Pi^{(\gamma)}_q(\omega) = \frac{1}{N} \sum_{k_1} \left| F_{\frac{q}{2}+k_1} F_{\frac{q}{2}-k_1} \right|^2 D^{(\gamma),(0)}_{q,k_1,k_1}(\omega), \tag{21}$$

in which the summation over k_1 runs over positive and negative values. The functions $\Pi^{(\gamma)}_q(\omega)$ can be regarded, apart from the product of form factors, as being equivalent to the various components of the "bare" or noninteracting two-phonon propagator. The imaginary parts of the Fourier transformed noninteracting propagator are nonzero at frequencies corresponding to the sum and difference of the frequencies for two harmonic phonons with total momentum q. The frequencies of the noninteracting two-phonon creation and the creation-annihilation excitations form continua in the (ω,q) phase space, as shown in Fig. 2. The common boundary separating the two-phonon sum and difference continua is marked by the red line decorated with triangles.

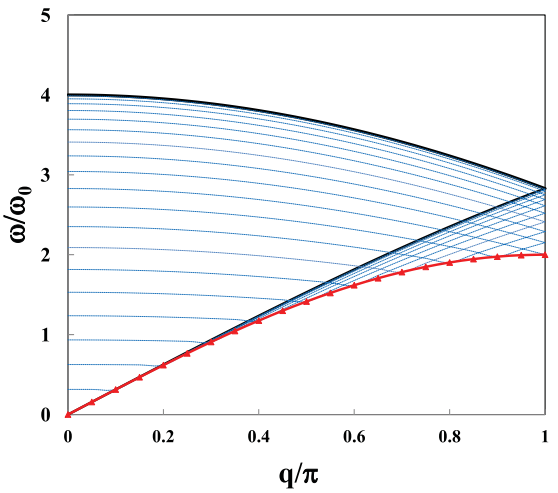

FIG. 2. (Color online) The (ω,q) phase space showing the extent of the continuum of two-phonon creation (shaded area). The continuum of Raman scattering excitations is located at frequencies immediately below the two-phonon creation continuum. The two continua are separated by the one-phonon dispersion relation, which is shown by the red line marked with triangles.

The solution of the coupled set of equations for the components of the interacting two-phonon propagator can be expressed as

$$D^{(\alpha),(\beta)}_{q,k,k'}(\omega) = D^{(\alpha),(0)}_{q,k,k}(\omega)\delta^{(\alpha),(\beta)}\Delta_{k-k'} + D^{(\alpha),(0)}_{q,k,k}(\omega) \times \frac{F^*_{\frac{q}{2}+k} F^*_{\frac{q}{2}-k} \left(\frac{2I_4}{N}\right) F_{\frac{q}{2}+k'} F_{\frac{q}{2}-k'}}{1 - I_4 \sum_\gamma \Pi^{(\gamma)}_q(\omega)} D^{(\beta),(0)}_{q,k',k'}(\omega). \tag{22}$$

In addition to having a dense set of poles that correspond to the two-phonon continua, the above expression may have poles at the frequencies at which the denominator vanishes:

$$1 - I_4 \sum_\gamma \Pi^{(\gamma)}_q(\omega) = 0. \tag{23}$$

Therefore, in addition to having poles within the two-phonon continua, the components of the two-phonon propagator (with fixed q) may also have poles at isolated frequencies that form a set of discrete dispersion relations. When the dispersion relations are located outside the continua, they describe long-lived collective breather excitations, since in this case the lifetime is determined by the imaginary parts of $\Pi^{(\gamma)}_q(\omega + i\eta)$, which vanish,

$$\sum_\gamma \mathrm{Im}\, \Pi^{(\gamma)}_q(\omega + i\eta) = 0, \tag{24}$$

when η is a positive infinitesimal quantity. If the dispersion relations are located within the continua, the imaginary parts

of $\Pi_q^{(\gamma)}(\omega + i\eta)$ are nonzero, so the collective excitations have finite lifetimes and exist only as resonances. Due to singularities in $\sum_\gamma \Pi_q^\gamma(\omega)$ (discussed in the Appendix A), both these collective modes are guaranteed to exist no matter how small the repulsive interaction I_4 is. The divergences in the two-phonon creation component are a consequence of the one-dimensional nature of the lattice. In three dimensions, one expects that the corresponding van Hove singularities would be washed out and that the collective modes would occur only for values of the anharmonicity exceeding a critical value. The $T = 0$ values of the dispersion relations for the collective modes agree with those previously found by another method [40], which allowed for the direct construction of the many-body wave function and demonstrated the localized nature of the excitations. Since the total number of phonons is not conserved, the collective mode is composed of a superposition of components from every channel. One sees that, at $T = 0$, each of the branches of collectives modes has a total weight of unity. Thus, the occurrence of breather excitations must be accompanied by a modification of the spectral weight in all the two-phonon continua. Since the total spectral weight is conserved at $T = 0$, one sees that Levinson's theorem [48] applies. Thus, we see that the determination of the $n = 2$ breather dispersion relation and spectral density for the β Fermi-Pasta-Ulam lattice requires the calculation of the noninteracting two-phonon propagators $\Pi_q^{(\alpha)}(\omega)$. This is discussed in Appendix A.

IV. THE α FERMI-PASTA-ULAM LATTICE

The Hamiltonian of the α Fermi-Pasta-Ulam lattice can be written in the second quantized form of

$$\hat{H} = \sum_q \frac{\hbar\omega_q}{2}(a_q^\dagger a_q + a_q a_q^\dagger) - i\frac{K_3}{3\sqrt{N}}\left(\frac{\hbar}{M\omega_0}\right)^{\frac{3}{2}} \times \sum_{k_1,k_2,k_3} \Delta_{k_1+k_2+k_3} \prod_{j=1}^{3} \left\{F_{k_j}\left(a_{k_j}^\dagger + a_{-k_j}\right)\right\}. \quad (25)$$

The interaction Hamiltonian has a separable form that has obvious similarities to the interaction Hamiltonian of the β lattice. However, it should be noted that the classical harmonic approximation to the ground state is metastable and is expected to become unstable when either the thermal and zero-point fluctuations are sufficiently large. This yields an upper limit to the strength of the anharmonic interaction for the approximate ground state to be long lived at $T = 0$, which is given by

$$I_3 \sim \hbar\omega_0, \quad (26)$$

where the interaction energy I_3 has been defined as

$$I_3 = K_3\left(\frac{\hbar}{M\omega_0}\right)^{\frac{3}{2}}. \quad (27)$$

Below this threshold, the approximate ground state is expected to decay with an exponentially small quantum tunneling rate.

The two-phonon spectra can be evaluated in a manner analogous to the method we used for the β lattice. The equations of motion for the two-phonon propagator can be truncated by approximating the time-ordered expectation value involving the equal-time commutators of the form

$$\left[\hat{A}_{q,k}^\alpha, \hat{H}_{\rm int}\right]. \quad (28)$$

The truncation can be performed by setting

$$\left[\hat{A}_{q,k}^\alpha, \hat{u}_{k_1}\hat{u}_{k_2}\hat{u}_{k_3}\right] \approx 3\left\langle\left[\hat{A}_{q,k}^\alpha, \hat{u}_{k_1}\hat{u}_{k_2}\right]\right\rangle \hat{u}_{k_3}, \quad (29)$$

in which the factor of 3 comes from the invariance of the commutator in expression (28) under the permutation of the indices of summation k_j. The truncated equations of motion for the components of the two-phonon propagator have the forms

$$\begin{aligned}\hbar\left(i\frac{\partial}{\partial t} \pm \omega_{\frac{q}{2}+k} \mp \omega_{\frac{q}{2}-k}\right) D_{q,k,k'}^{(\pm\mp),(\beta)}(t) &= -\delta(t)\left(\mp\left[\frac{1}{2} + N_{\frac{q}{2}+k}\right] \pm \left[\frac{1}{2} + N_{\frac{q}{2}-k}\right]\right)\Delta_{k-k'}\delta^{(\pm\mp),(\beta)} \\ &+ 2i\frac{I_3}{\sqrt{N}} F_{\frac{q}{2}+k}^* F_{\frac{q}{2}-k}^* F_q \left(\mp\left[\frac{1}{2} + N_{\frac{q}{2}+k}\right] \pm \left[\frac{1}{2} + N_{\frac{q}{2}-k}\right]\right) \sum_{\pm} G_{q,k'}^{\pm,(\beta)}(t), \end{aligned} \quad (30)$$

where we have introduced the anomalous propagators defined by

$$\begin{aligned} G_{q,k'}^{+,(\beta)}(t) &= -\frac{i}{\hbar}\left\langle \hat{T} a_q^\dagger(t) \hat{A}_{q,k}^{\beta\,\dagger}(0)\right\rangle, \\ G_{q,k'}^{-,(\beta)}(t) &= -\frac{i}{\hbar}\left\langle \hat{T} a_{-q}(t) \hat{A}_{q,k}^{\beta\,\dagger}(0)\right\rangle. \end{aligned} \quad (31)$$

The anomalous propagators involve only three phonon creation and annihilation operators, in contrast to the β lattice where the corresponding propagator involved four operators. The equations of motion for the anomalous propagators $G_{q,k'}^{\pm,\beta}(\omega)$ are of the form

$$\begin{aligned}\hbar\left(i\frac{\partial}{\partial t} \pm \omega_q\right) G_{q,k'}^{\pm,(\beta)}(t) &= \mp 2i\frac{I_3}{\sqrt{N}} F_q^* \sum_{\gamma,k''} F_{\frac{q}{2}+k''} F_{\frac{q}{2}-k''} D_{q,k'',k'}^{(\gamma)(\beta)}(t). \end{aligned} \quad (32)$$

On Fourier transforming the equations of motion for $G_{q,k'}^{\pm,(\beta)}(\omega)$ and after some manipulation, one finds that

$$\begin{aligned}\sum_{\pm} G_{q,k'}^{\pm,(\beta)}(\omega) &= 2i F_q^* \frac{2\hbar\omega_q}{\hbar^2\omega^2 - \hbar^2\omega_q^2}\frac{I_3}{\sqrt{N}} \\ &\times \sum_{\gamma,k''} F_{\frac{q}{2}+k''} F_{\frac{q}{2}-k''} D_{q,k'',k'}^{(\gamma)(\beta)}(\omega). \end{aligned} \quad (33)$$

The above equation, together with the Fourier transformed equations of motion,

$$\begin{aligned} D_{q,k,k'}^{(\alpha)(\beta)}(\omega) &= D_{q,k,k}^{(\alpha)(0)}(\omega)\delta^{(\alpha),(\beta)}\Delta_{k-k'} - 2i I_3 F_{\frac{q}{2}+k}^* F_{\frac{q}{2}-k}^* \\ &\times D_{q,k,k}^{(\alpha)(0)}(\omega) F_q \frac{1}{\sqrt{N}} \sum_{\pm} G_{q,k',k'}^{\pm,(\beta)}(\omega), \end{aligned} \quad (34)$$

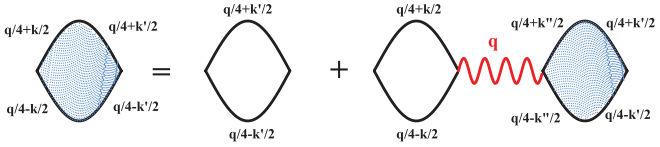

FIG. 3. (Color online) The Ladder Approximation to the two-particle Dyson equation for the α Fermi-Pasta-Ulam lattice. The interacting two-particle propagator is denoted by the shaded bubbles, and the noninteracting two-particle propagator is denoted by the open bubble. The interaction I_3 is represented by the vertex of a bubble connecting to the single-phonon propagator. The noninteracting single-phonon propagator with wave vector q, $D_q^{(0)}(\omega)$, is denoted by the red wavy line. The product of $2|\sin\frac{q}{2}|I_3 D_q^{(0)}(\omega) I_3$ acts as an effective wave vector and frequency-dependent interaction, $U_4(\omega,q)$.

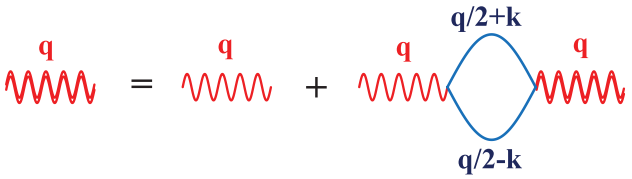

FIG. 4. (Color online) The single-particle Dyson equation for the α Fermi-Pasta-Ulam lattice. The interacting single-phonon propagators are denoted by the double red wavy lines, and the noninteracting single-phonon propagator is denoted by a single red wavy line. The noninteracting two-phonon propagator is denoted by the open bubble. The interaction I_3 is represented by the vertex of a bubble connecting to a single-phonon propagator.

forms a closed set of algebraic equations. This set of equations is recognized as describing the ladder approximation shown in Fig. 3. On eliminating $\sum_{\pm} G^{\pm,(\beta)}_{q,k'}(\omega)$, one finds

$$D^{(\alpha)(\beta)}_{q,k,k'}(\omega) = D^{(\alpha)(0)}_{q,k,k}(\omega)\delta^{(\alpha),(\beta)}\Delta_{k-k'} + F^*_{\frac{q}{2}+k}F^*_{\frac{q}{2}-k}D^{(\alpha)(0)}_{q,k,k}(\omega)\left[2|F_q|^2 I_3 \frac{2\hbar\omega_q}{\hbar^2\omega^2-\hbar^2\omega_q^2} I_3\right] \times \frac{2}{N}\sum_{\gamma,k''} F_{\frac{q}{2}+k''}F_{\frac{q}{2}-k''}D^{(\gamma),(\beta)}_{q,k'',k'}(\omega), \quad (35)$$

which maps onto Eq. (18) for the β lattice in which I_4 has been replaced by an effective frequency and wave vector-dependent interaction $U_4(\omega,q)$ defined by

$$U_4(\omega,q) = 2\left|\sin\frac{q}{2}\right| I_3 \frac{2\hbar\omega_q}{\hbar^2\omega^2-\hbar^2\omega_q^2} I_3, \quad (36)$$

which is a repulsive interaction for frequencies above the bare phonon frequency ω_q and is attractive for $\omega_q > \omega$. Hence, the solution for the components of the two-phonon propagator are found to be given by

$$D^{(\alpha)(\beta)}_{q,k,k'}(\omega) = D^{(\alpha)(0)}_{q,k,k}(\omega)\delta^{(\alpha),(\beta)}\Delta_{k-k'} + F^*_{\frac{q}{2}+k}F^*_{\frac{q}{2}-k}\frac{D^{(\alpha)(0)}_{q,k,k}(\omega)\frac{2U_4(\omega,q)}{N}D^{(\beta)(0)}_{q,k',k'}(\omega)}{1-U_4(\omega,q)\sum_\gamma \Pi^{(\gamma)}_q(\omega)} \times F_{\frac{q}{2}+k'}F_{\frac{q}{2}-k'}. \quad (37)$$

We note that, because of the frequency dependence of the effective interaction, the total (ω integrated) weight in the two-phonon spectral density is not conserved since weight is mixed into the single-phonon spectrum as can be seen from the single-phonon Dyson equation depicted in Fig. 4. The Fourier transform of the single-phonon propagator $D_q(t)$ defined by

$$D_q(t) = -\frac{i}{\hbar}\langle\hat{T}[a_q^\dagger(t)+a_{-q}(t)][a^\dagger_{-q}(0)+a_q(0)]\rangle \quad (38)$$

is calculated as

$$D_q(\omega) = \frac{2\hbar\omega_q}{\hbar^2\omega^2-\hbar^2\omega_q^2-2\hbar^2\omega_q^2\left(\frac{I_3^2}{\hbar\omega_0}\right)\sum_\gamma \Pi^{(\gamma)}_q(\omega)}. \quad (39)$$

This expression is in agreement with the general expressions deduced by Maradudin and Fein [37] and Cowley [38]. The polarization part of the single-phonon propagator renormalizes the single-phonon quasiparticle spectral density downward, introduces a broadened resonance just above the "bare" single-phonon frequency, and describes the isolated pole at the frequency of the $n = 2$ breather.

Like the β lattice, the two-phonon spectral density for the α lattice depends on the components of the noninteracting two-phonon propagator $\Pi^{(\gamma)}_q(\omega)$. However, for the α lattice, the renormalization of the single-phonon excitation energy and its decay rate is also determined by $\Pi^{(\gamma)}_q(\omega)$, which is given in Appendix A.

V. MONOATOMIC LATTICES: RESULTS AND DISCUSSION

A. The α lattice

The dispersion relation of the $n = 2$ breather and resonance can be obtained directly from the single-phonon propagator. This type of coupling between the single- and two-phonon continua was anticipated by Leath and Watson [42] over 40 years ago, although these authors were concerned neither with the Fermi-Pasta-Ulam model nor with breather excitations. The excitation energies are given by the solutions of the equation

$$\hbar^2\omega^2-\hbar^2\omega_q^2 = 4\hbar\omega_q I_3\left|\sin\frac{q}{2}\right| I_3\sum_\gamma \mathrm{Re}\,\Pi^{(\gamma)}_q(\omega). \quad (40)$$

The equation can be solved graphically by the intersection of the parabolic line with the polarization part as shown in Fig. 5. The decay rate of the excitations is given by the imaginary part of the polarization part at the intersection of the dashed parabola with the solid blue curve. It is seen that for a fixed q, there are three physically significant solutions. The lowest energy solution describes the renormalized phonon frequency. The phonon frequencies are softened, but due to the explicit factor of $|\sin\frac{q}{2}|$, the dispersion relation retains the linear form for low q values. At $T = 0$, both the $n = 2$ breather and the single-phonon excitations are described by delta functions with intensities given by

$$\left[1-2\left|\sin\frac{q}{2}\right| I_3^2\sum_\gamma \frac{\partial}{\partial\omega}\Pi^{(\gamma)}_q(\omega)\right]^{-1} \quad (41)$$

evaluated at their respective excitation energies. Since the slope of the real polarization part is negative at the intersections, the ω-integrated spectral weight associated with

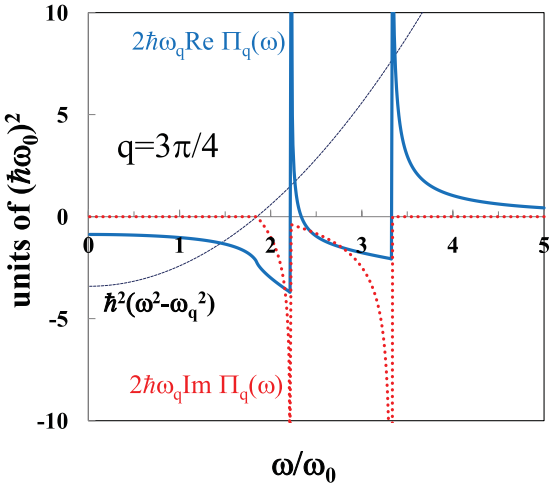

FIG. 5. (Color online) The graphical solution for the excitation energies for the renormalized single-phonon, the $n = 2$ resonance, and the $n = 2$ breather of the α lattice. The excitation energies are given by the intersection of the dashed parabolic curve $\hbar^2(\omega^2 - \omega_q^2)$ with $2\hbar\omega_q$ times the real part of the polarization part, $2|\sin\frac{q}{2}|I_3^2 \sum_\gamma \Pi_q^{(\gamma)}(\omega)$, shown by the solid blue line. The decay rate of each excitation is determined from the imaginary part (dotted red line) evaluated at the excitation energy. The interaction strength I_3 was set at $(\frac{I_3}{\hbar\omega_0}) = \frac{1}{\sqrt{2}}$.

each delta function is less than unity. The single-phonon spectral density is shown in Fig. 6.

The delta functions at the renormalized phonon frequency and at the $n = 2$ breather energy are marked by vertical lines. The lower threshold for the two-phonon continuum is given by the bare phonon frequency. The dispersion relation for the renormalized phonons, the $n = 2$ breather, and the resonance are shown in Fig. 7. It is expected that the renormalized phonon dispersion relation will become increasingly soft as the temperature or the interaction strength is increased, eventually

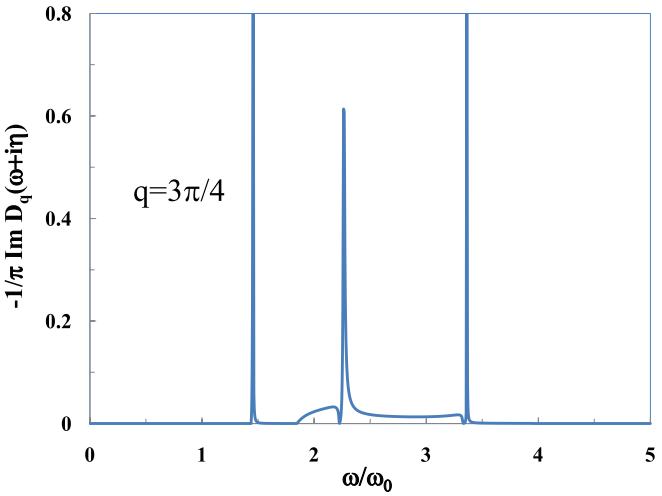

FIG. 6. (Color online) The $T = 0$ single-phonon spectral density, $-\frac{1}{\pi} D_q(\omega + i\eta)$, in units of $(\hbar\omega_0)^{-1}$, showing delta function peaks at the renormalized phonon frequency, the $n = 2$ breather, and a sharp resonance in the $n = 2$ continuum. The interaction I_3 has the same value as in Fig. 5.

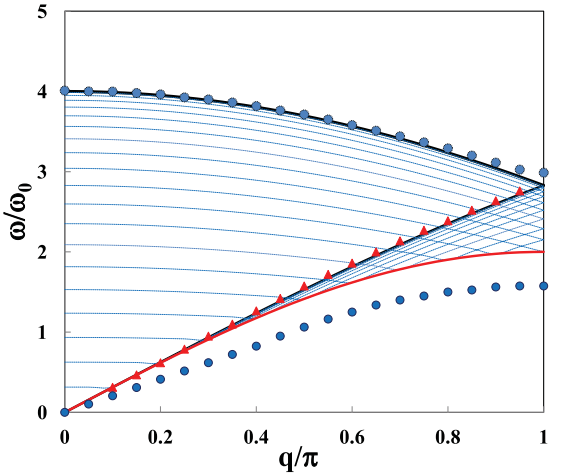

FIG. 7. (Color online) The dispersion relation for the renormalized phonons and the $n = 2$ breather of the α lattice are indicated by the filled blue circles. The position of the resonance is indicated by the filled red triangles. At $q = \pi$ the position of the $n = 2$ breather and the resonance become indistinguishable from the neighboring van Hove singularities in the noninteracting two-phonon continuum. The interaction I_3 has the same value as in Fig. 5.

reaching zero when the fluctuations become sufficiently large to drive the system unstable. For $T = 0$, our analysis suggests that the critical value of I_3 and the wave vector for the instability is given by the generalized Stoner criterion

$$0 = 1 + 2\hbar\omega_0 \left(\frac{I_3}{\hbar\omega_0}\right)^2 \sum_\gamma \Pi_q^{(\gamma)}(0). \tag{42}$$

At $T = 0$, this reduces to

$$1 = \frac{2}{\pi}\left(\frac{I_3}{\hbar\omega_0}\right)^2 \left[2 + \frac{\cos^2\frac{q}{4}}{2\sin\frac{q}{4}} \ln\left(\frac{1-\sin\frac{q}{4}}{1+\sin\frac{q}{4}}\right) + \frac{\sin^2\frac{q}{4}}{2\cos\frac{q}{4}} \ln\left(\frac{1-\cos\frac{q}{4}}{1+\cos\frac{q}{4}}\right)\right]. \tag{43}$$

The right-hand side is a mildly varying function of q, which has a broad maximum at $q = 0$, and suggests that the critical value of I_3 is given by

$$\left(\frac{I_3}{\hbar\omega_0}\right)^2 = \frac{\pi}{2}. \tag{44}$$

For I_3 close to this critical value, it is expected that the time scale for the decay of the approximate metastable state via large-amplitude tunneling fluctuations will be comparable to the decay rate produced via the (harmonic) zero-point fluctuations. Furthermore, for $(\frac{I_3}{\hbar\omega_0}) = 0.707$, one finds that as much as 10% of the $T = 0$ single-phonon spectral weight can be identified with the coupling to the two-phonon spectral density, and this percentage increases as I_3 increases. This is qualitatively consistent with the observation of Manley *et al.* that the breather excitation in NaI as measured in inelastic neutron-scattering experiments [36] is associated with an intensity proportional to Q^2, where Q is the neutron momentum transfer. This is consistent since the single-phonon spectral density $S(Q,\omega)$ measured in inelastic neutron-

scattering experiments [39] is related to the imaginary part of the single-phonon propagator via

$$S_1(Q,\omega) = -\frac{1}{2\pi^2}\exp[-W(Q)](\underline{Q}.\hat{\epsilon}_q)^2\left(\frac{\hbar}{2M\omega_q}\right) \times \mathrm{Im}D_q(\omega+i\eta)[1+N(\omega)], \quad (45)$$

where $W(Q)$ is the anharmonic analog of the Debye-Waller factor, q is the phonon wave vector, and $\hat{\epsilon}_q$ is the phonon polarization vector. Although there is no general nonperturbative theory of the Debye-Waller factor in the presence of anharmonic interactions [49], we note that for large values of I_3, the Debye-Waller factor is not simply given by the standard harmonic expression involving the renormalized phonon frequencies. This is due to the presence of the large admixture of the two-phonon spectra, which should also contribute to $W(Q)$. The appearance of the coupling proportional to Q^2 is in direct contrast to the results on the β lattice in which the only manifestation of the $n=2$ breather in the single-phonon spectrum is expected to be a weak broad peak. However, for the β lattice, the $n=2$ breather should show up directly as a sharp peak in the neutron scattering with a coupling strength proportional to Q^4.

B. The β lattice

The $n=2$ breather is expected to show up directly in the two-phonon spectrum as a sharp peak above the two-phonon continuum. The dispersion relation for the $n=2$ breather is shown in Fig. 8 at various temperatures. The breather spectrum for the β lattice has a finite separation for the two-phonon continuum for all q values. The $n=2$ breather and the $n=2$ resonance become strongly mixed at $q=\pi$. It is also seen that as the temperature increases, the energy separation of the breather excitation from the top of the two-phonon continuum

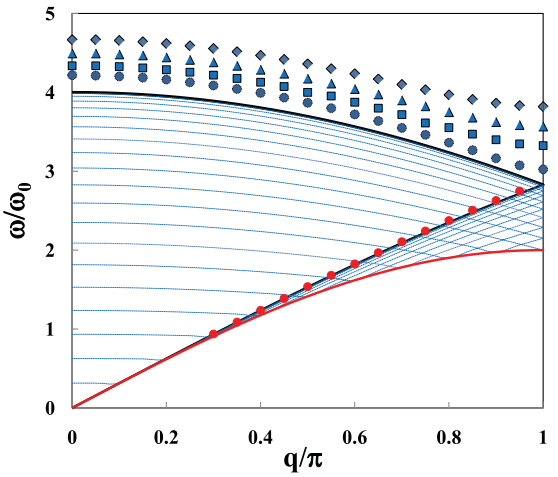

FIG. 8. (Color online) The dispersion relation for the $n=2$ resonance and the $n=2$ breather of the β lattice at the temperatures $(\frac{k_BT}{\hbar\omega_0}) = 0.0$ (blue circles), 1.0 (blue squares), 1.5 (blue triangles), and 2.0 (blue diamonds) with $(\frac{I_4}{\hbar\omega_0}) = 1$.

also increases, in accordance with the findings of Texeira Rabelo *et al.* [50]. The dispersion relation becomes flatter as the temperature increases consistent with the group velocity of the breather tending to zero in the classical limit. This finding is in accordance with the comments by Aubry [22], by Flach and Willis [23], and by Fleurov [51]. In contrast with the breather, the temperature-dependent shift of the excitation energy of the $n=2$ resonance has a much smaller magnitude.

Unlike the α lattice, the $n=2$ breather is not expected to show up in the single-phonon propagator. For the β lattice, the phonon polarization part is related to the three-phonon propagators, as depicted in Fig. 9. The single-phonon polarization part $\Pi_q(\omega)$ is calculated to second order in I_4 as

$$\Pi_q(\omega) = \frac{2I_4^2}{3N^2}\sum_{k_1,k_2}\left|\sin\frac{q}{2}\sin\left(\frac{q-k_1-k_2}{2}\right)\sin\frac{k_1}{2}\sin\frac{k_2}{2}\right|\left[\frac{2\hbar(\omega_{q-k_1-k_2}+\omega_{k_1}+\omega_{k_2})}{\hbar^2\omega^2-\hbar^2(\omega_{q-k_1-k_2}+\omega_{k_1}+\omega_{k_2})^2}\right] \times\left([1+N_{q-k_1-k_2}][1+N_{k_1}][1+N_{k_2}]-N_{q-k_1-k_2}N_{k_1}N_{k_2}\right) - \frac{2I_4^2}{N^2}\sum_{k_1,k_2}\left|\sin\frac{q}{2}\sin\left(\frac{q-k_1-k_2}{2}\right)\sin\frac{k_1}{2}\sin\frac{k_2}{2}\right| \times\left[\frac{2\hbar(-\omega_{q-k_1-k_2}+\omega_{k_1}+\omega_{k_2})}{\hbar^2\omega^2-\hbar^2(-\omega_{q-k_1-k_2}+\omega_{k_1}+\omega_{k_2})^2}\right]\left(N_{q-k_1-k_2}[1+N_{k_1}][1+N_{k_2}]-[1+N_{q-k_1-k_2}]N_{k_1}N_{k_2}\right). \quad (46)$$

When calculated to infinite order in I_4, the $n=2$ breather may be expected to appear in the polarization part in a convolution with a noninteracting single-phonon propagator and would at most give rise to a broad peak. However, from inspection of the polarization part given in Eq. (46), one is led to expect that for the β lattice, the single-phonon propagator will couple directly with the $n=3$ breather. The three-phonon creation continuum has van Hove singularities whose positions in the (k_1,k_2) plane are determined by the solutions of the simultaneous equations

$$\frac{\partial}{\partial_{k_1}}(\omega_{q-k_1-k_2}+\omega_{k_1}+\omega_{k_2})=0, \qquad \frac{\partial}{\partial_{k_2}}(\omega_{q-k_1-k_2}+\omega_{k_1}+\omega_{k_2})=0. \quad (47)$$

The critical points are located at $k_1=(\frac{q+2n\pi}{3})$ and $k_2=(\frac{q+2n\pi}{3})$ for $n=0,1$, and 2 cause the van Hove singularities

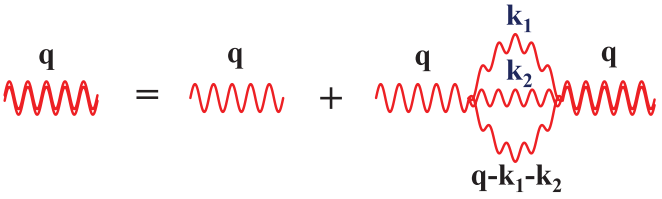

FIG. 9. (Color online) The Dyson equation for the single-phonon propagator for the β lattice. The dressed propagator is depicted by the double wavy lines, and the noninteracting propagator by the single wavy line. The lowest-order contribution to the single-phonon polarization part describes a coupling to three co-propagating phonons.

in the noninteracting three-phonon creation spectral density to have the form of discontinuities. The Kramers-Kronig relation relates the discontinuities in the imaginary part to logarithmic singularities in the real part. The divergences form bands in (ω,q) space, as seen in Fig. 10. In Fig. 11 it is seen that the second-order single-phonon polarization part exhibits a strong van Hove singularity at the top of the three-phonon creation continuum, which produces an isolated pole in the one-phonon spectrum. Due to the divergence at the van Hove singularities, the effect of multiple interactions between the three co-propagating phonons will produce a bound state above the three-phonon continuum, no matter how small the interaction strength I_4 is. This is a consequence of the one-dimensional nature of the model. Thus, the inclusion of multiple interactions is expected to produce a coupling of the single-phonon spectral density to the $n = 3$ breather. However, due to the large energy separation between the single-phonon energy and the top edge of the three-phonon continuum, the intensity of the $n = 3$ breather contribution to $S_1(Q,\omega)$ is expected to be relatively small. From this analysis, and the form of the van Hove singularities seen in Fig. 10, it should be clear that the resonances are analytic continuations of the breather excitations into the neighboring Brillouin zones.

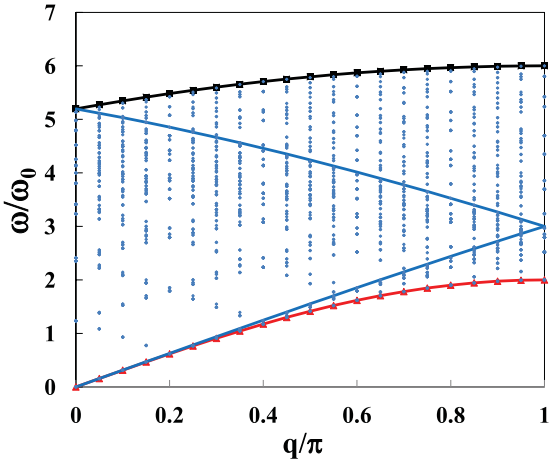

FIG. 10. (Color online) The positions of the van Hove singularities of the three-phonon creation continuum, in (ω,q) space, are marked by the black and blue solid lines. The continuum is bounded from above by the black solid line decorated with squares and is bounded from below by the single-phonon dispersion relation (red line with triangles).

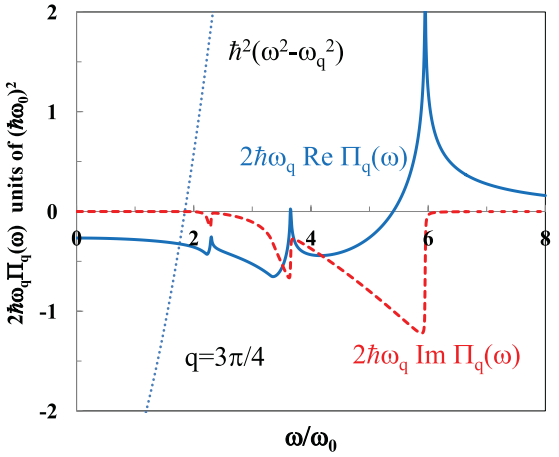

FIG. 11. (Color online) The real (blue) and imaginary (red) parts of $2\hbar\omega_q$ times the $T = 0$ phonon polarization part $\Pi_q(\omega)$ for the β lattice (in units of $\hbar^2\omega_0^2$) evaluated at $q/\pi = 3/4$ with $(\frac{I_4}{\hbar\omega_0}) = 1$. The polarization part exhibits a strong van Hove singularity at the top of the three-phonon creation continuum. The real part of the polarization part is expected to diverge logarithmically at the singularities; however, the results shown here do not diverge due to numerical rounding. The dashed blue parabola represents $\hbar^2(\omega^2 - \omega_q^2)$. The energy of the $n = 3$ breather is expected to be found at the intersection of the blue curves at frequencies above the three-phonon continuum.

VI. THE HAMILTONIAN OF THE DIATOMIC FERMI-PASTA-ULAM LATTICE

The diatomic Fermi-Pasta-Ulam lattice consists of an alternating periodic array of atoms with masses M_A and M_B, as shown in Fig. 12, which are coupled by harmonic and anharmonic nearest-neighbor interactions. The anharmonic Hamiltonian for the lattice is given by

$$\hat{H} = \sum_i \left(\frac{\hat{P}_{i,A}^2}{2M_A} + \frac{\hat{P}_{i,B}^2}{2M_B} \right) + \frac{K_2}{2} \sum_i [(\hat{u}_{i,A} - \hat{u}_{i,B})^2 + (\hat{u}_{i,B} - \hat{u}_{i+1,A})^2] + \frac{K_4}{12} \sum_i [(\hat{u}_{i,A} - \hat{u}_{i,B})^4 + (\hat{u}_{i,B} - \hat{u}_{i+1,A})^4], \quad (48)$$

where the index i labels the unit cell. The first line represents the harmonic part of the Hamiltonian, and the second line (proportional to K_4) represents the anharmonic interaction. It should be noted that the Hamiltonian is symmetric under the continuous transformation $u_{i,A} \to u_{i,A} + \delta$ and $u_{i,B} \to u_{i,B} + \delta$; thus we have assumed that the continuous symmetry of the ground state has been spontaneously broken. The spontaneously broken symmetry of the ground state is

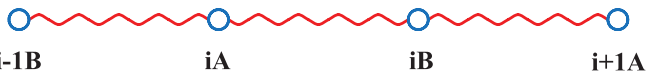

FIG. 12. (Color online) A cartoon of a four atom segment of the diatomic Fermi-Pasta-Ulam lattice, in which atoms of masses M_A and M_B are arranged periodically on alternating sites.

responsible for the occurrence of a branch of Goldstone modes.

In Appendix B, the harmonic part of the Hamiltonian $\hat{H}_0$ is written in terms of the Fourier transformed phonon creation and annihilation operators, $\gamma^\dagger_{j,q}$ and $\gamma_{j,q}$, respectively, for the optic and acoustic phonon ($j = 1, 2$) bands as

$$\hat{H}_0 = \sum_q \frac{\hbar\omega_{1,q}}{2}(\gamma^\dagger_{1,q}\gamma_{1,q} + \gamma_{1,q}\gamma^\dagger_{1,q}) + \sum_q \frac{\hbar\omega_{2,q}}{2}(\gamma^\dagger_{2,q}\gamma_{2,q} + \gamma_{2,q}\gamma^\dagger_{2,q}), \tag{49}$$

where the dispersion relations are given by

$$\omega^2_{j,q} = K_2\left(\frac{1}{M_A} + \frac{1}{M_B}\right)\left[1 \pm \sqrt{1 - \frac{4M_AM_B}{(M_A + M_B)^2}\sin^2\frac{q}{2}}\right] \tag{50}$$

in which the optical branch ($j = 1$) corresponds to the positive sign and the acoustic branch ($j = 2$) corresponds to the negative sign. The dispersion relations for the acoustic and optic branches of the phonon excitations are shown in Fig. 13.

The anharmonic interaction $\hat{H}_{\rm int}$ can be written in the form of a sum of two separable momentum-conserving interactions. In Appendix B the interaction is put into the second quantized form

$$\hat{H}_{\rm int} = \left(\frac{K_4\hbar^2}{48N}\right)\sum_{m=1}^{2}\left[\sum_{k_1,k_2,k_3,k_4}\Delta_{k_1+k_2+k_3+k_4} \times \prod_{j=1}^{4}\left\{\sum_{i=1}^{2}F^{(m)}_{i,k_j}\left(\gamma^\dagger_{i,k_j} + \gamma_{i,-k_j}\right)\right\}\right], \tag{51}$$

where the form factors for each separable interaction $F^{(m)}_{i,k}$ are complex numbers that are given in Appendix B.

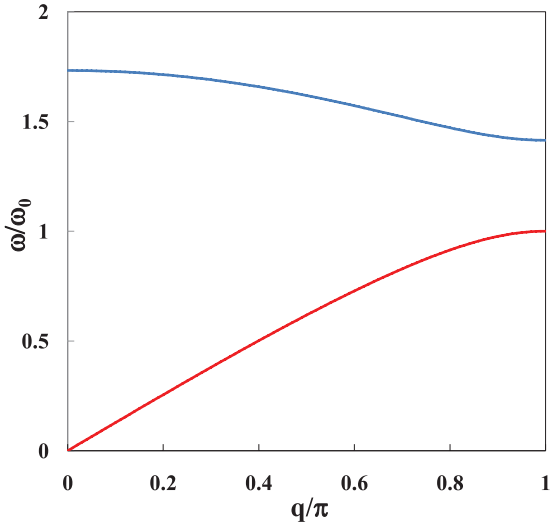

FIG. 13. (Color online) The acoustic and optic branches of the dispersion relation for the diatomic harmonic lattice with $M_B = 2M_A$. A characteristic frequency ω_0 has been defined in terms of the harmonic force constant K_2 via $K_2 = M_A\omega_0^2$.

VII. DIATOMIC LATTICE: THE LADDER APPROXIMATION

The two-phonon propagator can be evaluated in the ladder approximation depicted in Fig. 1. By Fourier transforming the equations of motion and using a generalization of the notation of Ref. [40], the two-particle Dyson equation can be expressed as

$$D^{(\alpha)(\alpha')}_{q,k,k'}(\omega) = D^{(\alpha)(0)}_{q,k,k}(\omega)(\delta^{(\alpha)(\alpha')}\Delta_{k-k'} + \delta^{(\tilde{\alpha})(\alpha')}\Delta_{k+k'}) + \frac{1}{N}\sum_{m=1}^{2}D^{(\alpha)(0)}_{q,k,k}(\omega)\left(H^{(m)}_{\alpha,q,k}\right)^* J_4 \times \sum_{\beta,k''}H^{(m)}_{\beta,q,k''}D^{(\beta)(\alpha')}_{q,k'',k'}(\omega), \tag{52}$$

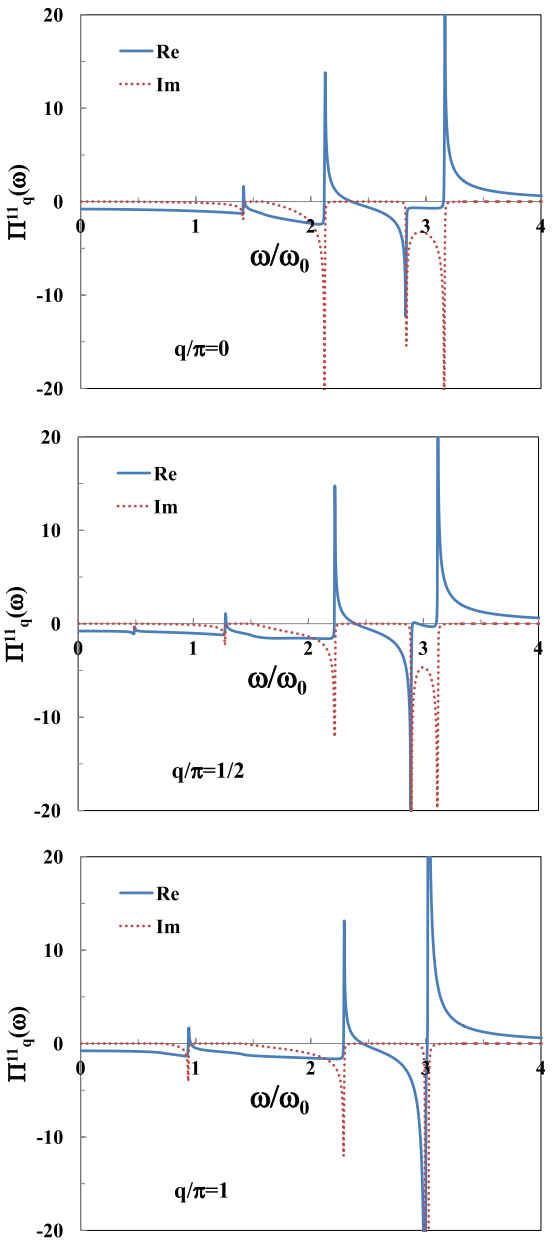

FIG. 14. (Color online) The ω dependence of the real (blue solid line) and imaginary parts (red dotted line) of $\Pi^{11}_q(\omega + i\eta)$ for various q values. The polarization parts are evaluated with $M_B = 4M_A$.

where the index (α) denotes the pairs of indices $(\pm,i;\pm,j)$ that describe the two-phonon operators so that the $\pm$ denotes either the creation or annihilation operator and the Latin index i denotes either the optic $(i=1)$ or the acoustic $(i=2)$ phonon mode. The index $(\tilde{\alpha})$ represents the transpose of the pair of excitations denoted by the index (α). The noninteracting two-phonon propagators $D^{(\alpha)(0)}_{q,k,k}(\omega)$ are diagonal in the pair of indices k,k' and $(\alpha),(\alpha')$ and are given by

$$D^{(\alpha)(0)}_{q,k,k}(\omega)=\frac{\pm\left(\frac{1}{2}+N_{i,\frac{q}{2}+k}\right)\pm\left(\frac{1}{2}+N_{j,\frac{q}{2}-k}\right)}{\hbar\left(\omega\mp\omega_{i,\frac{q}{2}+k}\mp\omega_{j,\frac{q}{2}-k}\right)}. \tag{53}$$

The factor $\pm$ multiplying the factor $(\frac{1}{2}+N_{i,\frac{q}{2}+k})$ should be associated with the phonon mode with index j and momentum $\frac{q}{2}-k$, and the sign in front of $(\frac{1}{2}+N_{j,\frac{q}{2}-k})$ corresponds to the mode labeled by the index i and the momentum $\frac{q}{2}+k$. The factors $H^{(m)}_{\alpha,q,k}$ are dimensionless complex numbers that represent the product of the form factors for the pair of excitations

$$H^{(m)}_{\alpha,q,k}=\left(\frac{K_2}{\omega_0}\right)F^{(m)}_{i,\frac{q}{2}+k}F^{(m)}_{j,\frac{q}{2}-k} \tag{54}$$

involved in the mth component of the interaction. The interaction strength J_4 has units of energy and is given by

$$J_4=\left(\frac{K_4\hbar^2\omega_0^2}{4K_2^2}\right). \tag{55}$$

The set of algebraic equations represented by (52) form a closed set. On introducing the set of functions denoted by

$$\begin{aligned}\Pi^{mm'}_q(\omega)=&\frac{1}{N}\sum_{k,i,j}H^{(m)}_{i,j,q,k}\frac{2\hbar\left(\omega_{i,\frac{q}{2}+k}+\omega_{j,\frac{q}{2}-k}\right)\left(1+N_{i,\frac{q}{2}+k}+N_{j,\frac{q}{2}-k}\right)}{\hbar^2\omega^2-\hbar^2\left(\omega_{i,\frac{q}{2}+k}+\omega_{j,\frac{q}{2}-k}\right)^2}\left(H^{(m')}_{i,j,q,k}\right)^*\\&+\frac{1}{N}\sum_{k,i,j}H^{(m)}_{i,j,q,k}\frac{2\hbar\left(\omega_{i,\frac{q}{2}+k}-\omega_{j,\frac{q}{2}-k}\right)\left(N_{j,\frac{q}{2}-k}-N_{i,\frac{q}{2}+k}\right)}{\hbar^2\omega^2-\hbar^2\left(\omega_{i,\frac{q}{2}+k}-\omega_{j,\frac{q}{2}-k}\right)^2}\left(H^{(m')}_{i,j,q,k}\right)^*,\end{aligned} \tag{56}$$

one finds that the two-phonon propagators can be expressed as

$$\begin{aligned}D^{(\alpha)(\alpha')}_{q,k,k'}(\omega)=&D^{(\alpha)(0)}_{q,k,k}(\omega)(\delta^{(\alpha)(\alpha')}\Delta_{k-k'}+\delta^{(\tilde{\alpha})(\alpha')}\Delta_{k+k'})\\&+2D^{(\alpha)(0)}_{q,k,k}(\omega)\frac{\left(H^{(1)}_{\alpha,q,k}\right)^*J_4\left[1-J_4\Pi^{22}_q(\omega)\right]H^{(1)}_{\alpha',q,k''}}{\left[1-J_4\Pi^{11}_q(\omega)\right]\left[1-J_4\Pi^{22}_q(\omega)\right]-J_4^2\Pi^{12}_q(\omega)\Pi^{21}_q(\omega)}D^{(\alpha')(0)}_{q,k',k'}(\omega)\\&+2D^{(\alpha)(0)}_{q,k,k}(\omega)\frac{\left(H^{(1)}_{\alpha,q,k}\right)^*J_4^2\Pi^{12}_q(\omega)H^{(2)}_{\alpha',q,k''}}{\left[1-J_4\Pi^{11}_q(\omega)\right]\left[1-J_4\Pi^{22}_q(\omega)\right]-J_4^2\Pi^{12}_q(\omega)\Pi^{21}_q(\omega)}D^{(\alpha')(0)}_{q,k',k'}(\omega)\\&+2D^{(\alpha)(0)}_{q,k,k}(\omega)\frac{\left(H^{(2)}_{\alpha,q,k}\right)^*J_4\left[1-J_4\Pi^{11}_q(\omega)\right]H^{(2)}_{\alpha',q,k''}}{\left[1-J_4\Pi^{11}_q(\omega)\right]\left[1-J_4\Pi^{22}_q(\omega)\right]-J_4^2\Pi^{12}_q(\omega)\Pi^{21}_q(\omega)}D^{(\alpha')(0)}_{q,k',k'}(\omega)\\&+2D^{(\alpha)(0)}_{q,k,k}(\omega)\frac{\left(H^{(2)}_{\alpha,q,k}\right)^*J_4^2\Pi^{21}_q(\omega)H^{(1)}_{\alpha',q,k''}}{\left[1-J_4\Pi^{11}_q(\omega)\right]\left[1-J_4\Pi^{22}_q(\omega)\right]-J_4^2\Pi^{12}_q(\omega)\Pi^{21}_q(\omega)}D^{(\alpha')(0)}_{q,k',k'}(\omega).\end{aligned} \tag{57}$$

The factor of two comes from the degeneracy of the bosonic two-particle propagator due to the permutation of the operators.

VIII. DIATOMIC LATTICE: THE TWO-PHONON POLARIZATION PARTS

The two-phonon polarization parts satisfy

$$\Pi^{11}_q(\omega)=\Pi^{22}_q(\omega) \tag{58}$$

and

$$\Pi^{12}_q(\omega)=\Pi^{21}_q(\omega^*)^* \tag{59}$$

for complex frequencies ω. The diagonal components are found to be given by

$$\begin{aligned}\Pi^{11}_q(\omega)=&\frac{1}{N}\sum_{k,i,j}\left(\frac{\omega_{i,\frac{q}{2}+k}\omega_{j,\frac{q}{2}-k}}{4\omega_0^2}\right)\frac{2\hbar\left(\omega_{i,\frac{q}{2}+k}+\omega_{j,\frac{q}{2}-k}\right)\left(1+N_{i,\frac{q}{2}+k}+N_{j,\frac{q}{2}-k}\right)}{\hbar^2\omega^2-\hbar^2\left(\omega_{i,\frac{q}{2}+k}+\omega_{j,\frac{q}{2}-k}\right)^2}\\&+\frac{1}{N}\sum_{k,i,j}\left(\frac{\omega_{i,\frac{q}{2}+k}\omega_{j,\frac{q}{2}-k}}{4\omega_0^2}\right)\frac{2\hbar\left(\omega_{i,\frac{q}{2}+k}-\omega_{j,\frac{q}{2}-k}\right)\left(N_{j,\frac{q}{2}-k}-N_{i,\frac{q}{2}+k}\right)}{\hbar^2\omega^2-\hbar^2\left(\omega_{i,\frac{q}{2}+k}-\omega_{j,\frac{q}{2}-k}\right)^2}.\end{aligned} \tag{60}$$

The real and imaginary parts of $\Pi_q^{11}(\omega + i\eta)$ where $\eta \to 0$ are shown in Fig. 14 for various q values. The imaginary parts are nonzero with the two-phonon creation continua and vanish elsewhere. The extent of the two-phonon creation continua are shown in Fig. 15. The real and imaginary parts exhibit divergent van Hove singularities at most of the extrema of the two-phonon continua. The divergencies shown in the figure are suppressed due to limited numerical accuracy. The notable exceptions to the divergent behavior are found at the lower edges of the acoustic-mode two-phonon continuum and the mixed-mode continuum since the form factors vanish there. The off-diagonal polarization parts $\Pi_q^{12}(\omega)$ also simplify, since the complex products of the form factors are given by the expressions

$$\frac{K_2}{\omega_0} F_{j,k}^{(1)} F_{j,k}^{(2)*} = (-1)^j \left(\frac{\omega_{j,k}}{2\omega_0}\right) \left[\frac{\cos\frac{k}{2}\left(\frac{1}{M_A}+\frac{1}{M_B}\right) - i\sin\frac{k}{2}\left(\frac{1}{M_A}-\frac{1}{M_B}\right)}{\sqrt{\left(\frac{1}{M_A}+\frac{1}{M_B}\right)^2 - \frac{4}{M_A M_B}\sin^2\frac{k}{2}}}\right] \tag{61}$$

so that the contributions to $\Pi_q^{12}(\omega)$ from the imaginary parts of the product vanish. This follows since the contributions are antisymmetric under the permutation $(i, \frac{q}{2}+k) \leftrightarrow (j, \frac{q}{2}-k)$, and, therefore, the imaginary part vanishes when the summations over k and (i,j) are performed. Thus, one has

$$\begin{aligned}\Pi_q^{12}(\omega) = {} & \frac{1}{N}\sum_{k,i,j}(-1)^{i+j} R_{q,k}\left(\frac{\omega_{i,\frac{q}{2}+k}\omega_{j,\frac{q}{2}-k}}{4\omega_0^2}\right)\frac{2\hbar\left(\omega_{i,\frac{q}{2}+k}+\omega_{j,\frac{q}{2}-k}\right)\left(1+N_{i,\frac{q}{2}+k}+N_{j,\frac{q}{2}-k}\right)}{\hbar^2\omega^2-\hbar^2\left(\omega_{i,\frac{q}{2}+k}+\omega_{j,\frac{q}{2}-k}\right)^2} \\ & + \frac{1}{N}\sum_{k,i,j}(-1)^{i+j} R_{q,k}\left(\frac{\omega_{i,\frac{q}{2}+k}\omega_{j,\frac{q}{2}-k}}{4\omega_0^2}\right)\frac{2\hbar\left(\omega_{i,\frac{q}{2}+k}-\omega_{j,\frac{q}{2}-k}\right)\left(N_{j,\frac{q}{2}-k}-N_{i,\frac{q}{2}+k}\right)}{\hbar^2\omega^2-\hbar^2\left(\omega_{i,\frac{q}{2}+k}-\omega_{j,\frac{q}{2}-k}\right)^2},\end{aligned} \tag{62}$$

where the dimensionless factor $R_{q,k}$ is given by

$$R_{q,k} = \frac{\cos k\left(\frac{1}{M_A^2}+\frac{1}{M_B^2}\right) + \cos\frac{q}{2}\left(\frac{2}{M_A M_B}\right)}{\sqrt{\left(\frac{1}{M_A}+\frac{1}{M_B}\right)^2 - \frac{4}{M_A M_B}\sin^2\left(\frac{q+2k}{4}\right)}\sqrt{\left(\frac{1}{M_A}+\frac{1}{M_B}\right)^2 - \frac{4}{M_A M_B}\sin^2\left(\frac{q-2k}{4}\right)}}. \tag{63}$$

The real and imaginary parts of $\Pi_q^{11}(\omega + i\eta)$ where $\eta \to 0$ are shown in Fig. 16 for various q values. Due to the factor $R_{q,k}$, the imaginary part of the function $\Pi_q^{12}(\omega + i\eta)$ changes sign for frequencies between the extrema of the acoustic two-phonon continuum at $k = 0$ and the upper edge where $k = \pi$. Since the k values of the extrema are reversed for the optic two-phonon continuum, the pattern of signs is opposite for the acoustic and optic continua. In the limit $q \to \pi$, there is a confluence of the energies of the $k = 0$ and $k = \pi$ extrema, which results in cancellation so that the function $\Pi_\pi^{12}(\omega)$ vanishes.

IX. DIATOMIC LATTICE: RESULTS AND DISCUSSION

The $n = 2$ breather and resonance energies are given by the solutions of the equation

$$\mathrm{Re}\left\{\left[1 - J_4\Pi_q^{11}(\omega)\right]\left[1 - J_4\Pi_q^{22}(\omega)\right] - J_4^2\Pi_q^{12}(\omega)\Pi_q^{21}(\omega)\right\} = 0. \tag{64}$$

The dispersion relation for the long-lived breathers are given by the solutions for which the corresponding imaginary parts are identically zero, i.e.,

$$\mathrm{Im}\left\{\left[1 - J_4\Pi_q^{11}(\omega)\right]\left[1 - J_4\Pi_q^{22}(\omega)\right] - J_4^2\Pi_q^{12}(\omega)\Pi_q^{21}(\omega)\right\} = 0. \tag{65}$$

Therefore, the breather excitations must have dispersion relations that are located outside the regions of (ω,q) phase space occupied by the two-phonon continua. At zero temperatures, these regions are shown in Fig. 15. The solutions of Eqs. (64) and (65) are shown by the solid lines marked by the filled circles. The dispersion relations lie above the top edges of the various two-phonon continua, and the energy separation between the branches of $n = 2$ breathers and the continua are seen to increase as one moves to the successive higher-energy branches. The increasing energy separations are correlated with decreasing widths of the successive two-phonon continua. It is also seen that the dispersion relation of the breathers become successively flatter for the higher-energy branches, which is in agreement with the findings of Wang *et al.* [27] for the quantum breathers of the ϕ^4 lattice. This is supportive of the argument of Fleurov [51], which suggests that classical breathers should be localized; however, quantum breathers may move by quantum mechanical tunneling. Hence, the band widths should decrease for the higher-energy branches as the classical limit is approached. The position of the lowest energy breather is found at energies above the dispersion relation for the acoustic phonon and below the optic phonon dispersion relation. This is in agreement with the inelastic neutron-scattering results of Manley *et al.* [36] on three-dimensional NaI in which they found a sharp spectral feature between the acoustic and optic phonon branches.

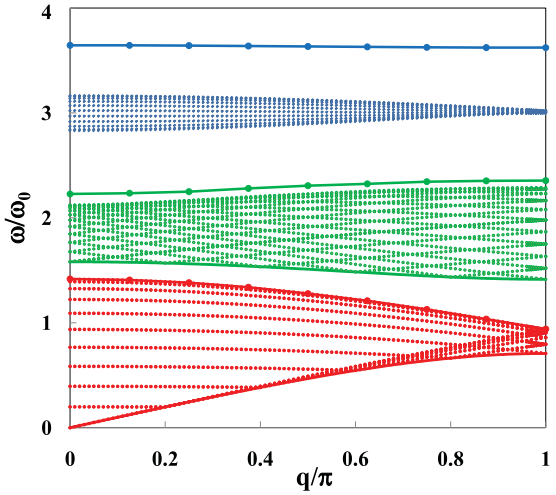

FIG. 15. (Color online) The (ω,q) phase-space map of the acoustic (lower band = red shading), mixed mode (middle band + green shading), and optic (upper band = blue shading) two-phonon creation continua for the diatomic harmonic lattice, with $M_B = 4M_A$. For sufficiently large mass differences ($M_B > 3M_A$), the gap between the acoustic and mixed mode continua extends across the entire Brillouin zone, while for smaller values of the mass differences ($3M_A > M_B > M_A$), the mixed mode and acoustic continua merge and have some overlap for small q values. The dispersion relations for the $n = 2$ breather excitations defined by the solutions of Eqs. (64) and (65) are marked by the solid lines decorated with the full circles. The dispersion relations for the harmonic phonon are marked by the full lines and coincide with the lower edges of the two lowest energy two-phonon continua.

X. CONCLUSIONS

In summary, we have shown that the quantized Fermi-Pasta-Ulam lattices have intrinsically nonlinear excitations that exist as breathers or resonances, no matter how weak the interaction strength is. Furthermore, we have shown that the $n = 2$ and 3 breather excitations could be expected to show up in inelastic neutron-scattering experiments through the single-phonon scattering cross section, due to the presence of a cubic component to the anharmonic interaction. This could also be expected to be true for more general forms of the anharmonic interactions and is consistent with experimental observations [36]. In particular, the experiments demonstrate the existence of a sharp feature with a fairly flat dispersion relation that lies in the gap between the acoustic and optic phonon branches, as found for the diatomic lattice. The intensity of the sharp feature is proportional to Q^2, indicating that this component involves coupling to the single-phonon spectrum. However, the coupling of the nonlinear excitations to the single-phonon spectra is not expected to extend to larger values of n, if the anharmonic interactions are weak. This expectation is based on the observation that the van Hove singularities in the noninteracting n-phonon continua have the form of van Hove singularities in the density of states of an $(n-1)$-dimensional system and, therefore, are only expected to give rise to either divergences or discontinuities for $n = 2$ and 3. For larger values of n, one expects that the van Hove singularities will take the form of either extremal points or points of inflection.

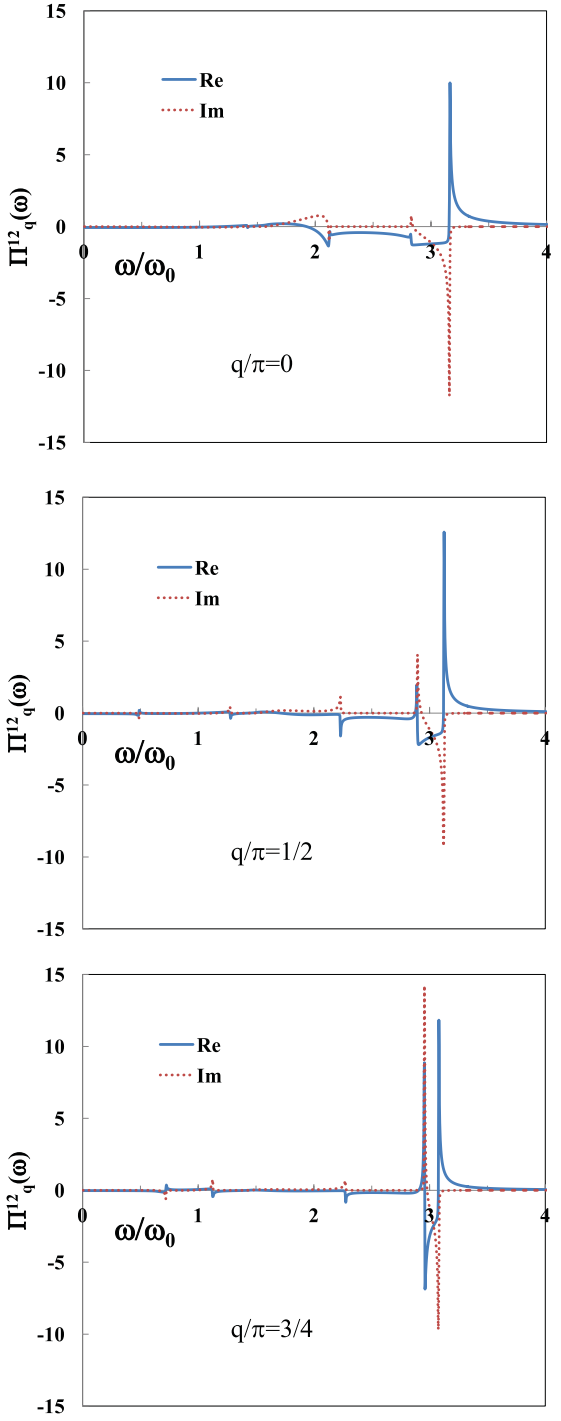

FIG. 16. (Color online) The ω dependence of the real and imaginary parts of $\Pi_q^{12}(\omega + i\eta)$ for various q values. The polarization parts are evaluated with $M_B = 4M_A$.

It is the divergences in the real part of the noninteracting $n = 2$ or 3 multiphonon propagators that are responsible for the formation of the breathers and the resonances at arbitrarily small interaction strengths, and it is these divergences that also give rise to the coupling with the single-phonon scattering cross section.

Since the van Hove singularities do not diverge in three spatial dimensions, one expects that a critical value of the

anharmonic interaction has to be exceeded before the $n = 2$ breather is formed. The presence of the Bose-Einstein distribution function n the polarization part multiplying the anharmonicity has the effect of enhancing the effective interactions at high temperatures and could be expected to lead to the appearance of the $n = 2$ breather in NaI at temperatures above a critical temperature. This expectation is consistent with experiment, since the sharp feature was only observed at $T = 555$ K and since the feature was not observed in experiments carried out below $T = 438$ K.

ACKNOWLEDGMENTS

This work was supported by the US Department of Energy, Office of Basic Energy Sciences, Materials Science through the award DEFG02-84ER45872. The author thanks A. R. Bishop, D. K. Campbell, S. Flach, J. C. Lasley, G. E. Lander, M. E. Manley, and A. J. Sievers for stimulating conversations.

APPENDIX A

Analytic expressions for the real and imaginary parts of the $T = 0$ two-phonon creation components of the propagator for the monoatomic lattice are discussed in this Appendix.

The imaginary parts of the components of the two-phonon propagator are given by

$$\begin{aligned}&\mathrm{Im}\,\Pi_q^{(\alpha)}(\omega + i\eta)\\ &= -\frac{\pi}{\hbar}\int_{-\pi}^{\pi}\frac{dk}{2\pi}\delta\left(\omega \mp \omega_{\frac{q}{2}+k} \pm \omega_{\frac{q}{2}-k}\right)\left|F_{\frac{q}{2}+k}F_{\frac{q}{2}-k}\right|^2\\ &\quad\times\left[\pm\left(\frac{1}{2}+N_{\frac{q}{2}+k}\right)\mp\left(\frac{1}{2}+N_{\frac{q}{2}-k}\right)\right],\end{aligned}\tag{A1}$$

where the sum over k has been replaced by an integral over k. The integration can be performed by using the properties of the delta function, yielding

$$\begin{aligned}\mathrm{Im}\,\Pi_q^{(\alpha)}(\omega + i\eta) = -\frac{1}{2\hbar}\sum_k \frac{\left|F_{\frac{q}{2}+k}F_{\frac{q}{2}-k}\right|^2}{\left|\frac{\partial}{\partial k}\left(\pm\omega_{\frac{q}{2}+k}\mp\omega_{\frac{q}{2}-k}\right)\right|}\\ \times\left[\pm\left(\frac{1}{2}+N_{\frac{q}{2}+k}\right)\mp\left(\frac{1}{2}+N_{\frac{q}{2}-k}\right)\right],\end{aligned}\tag{A2}$$

where the sum over k is restricted to the values that are the solutions of

$$\omega = \pm\omega_{\frac{q}{2}+k} \mp \omega_{\frac{q}{2}-k}.\tag{A3}$$

For general values of q, the imaginary part of the components of the "bare" two-phonon propagator are expected to be singular at the boundaries [52]. At the boundaries, the imaginary part may become infinite, since the boundaries are defined by the k values for which $\pm\omega_{\frac{q}{2}+k} \mp \omega_{\frac{q}{2}-k}$ is extremal. For example, for $0 < q < \pi$, the upper edges of two-phonon creation continuum is given by

$$4\omega_0 \cos\frac{q}{4},\tag{A4}$$

and this maximal value corresponds to $k = \pi$. In the region of (ω,q) given by

$$4\omega_0 \cos\frac{q}{4} > \omega > 4\omega_0 \sin\frac{q}{4},\tag{A5}$$

the imaginary part of the two-phonon creation continuum is nonzero and is determined by the equivalent k values with a magnitude found from

$$\omega = 4\omega_0 \cos\frac{q}{4}\sin\frac{k}{2},\tag{A6}$$

which leads to a square root divergence at the upper boundary of the continuum with the form

$$\begin{aligned}&\mathrm{Im}\,\Pi_q^{(++)}(\omega + i\eta)\\ &\propto -\frac{2}{\hbar\sqrt{16\omega_0^2\cos^2\frac{q}{4}-\omega^2}}\frac{\left|\omega^2 - 4\omega_0^2\sin^2\frac{q}{2}\right|}{16{\omega_0}^2\cos^2\frac{q}{4}},\end{aligned}\tag{A7}$$

when $4\omega_0 \cos\frac{q}{4} > \omega$, and is zero otherwise. The Bose-Einstein distribution functions in the factor $[1 + N_{\frac{q}{2}+k} + N_{\frac{q}{2}-k}]$ (not displayed) are evaluated at the frequencies given by

$$\omega_{\frac{q}{4}\pm\frac{k}{2}} = \frac{1}{2}\left[\omega \pm \tan\frac{q}{4}\sqrt{16\omega_0^2\cos^2\frac{q}{4}-\omega^2}\right].\tag{A8}$$

For values of (ω,q) that satisfy the inequality

$$4\omega_0 \sin\frac{q}{4} > \omega > 2\omega_0 \sin\frac{q}{2},\tag{A9}$$

the imaginary part of the two-phonon creation component of the propagator is determined by the equivalent k values with magnitudes that satisfy either of the equations

$$\begin{aligned}\omega &= 4\omega_0 \cos\frac{q}{4}\sin\frac{k}{2} \quad \text{for} \quad k \geqslant \frac{q}{2},\\ \omega &= 4\omega_0 \sin\frac{q}{4}\cos\frac{k}{2} \quad \text{for} \quad k \leqslant \frac{q}{2}.\end{aligned}\tag{A10}$$

The corresponding phonon frequencies that enter the factor $[1 + N_{\frac{q}{2}-k} + N_{\frac{q}{2}-k}]$ containing the Bose-Einstein distribution functions are given by

$$\begin{aligned}\omega_{\frac{q}{4}\pm\frac{k}{2}} &= \frac{1}{2}\left[\omega \pm \tan\frac{q}{4}\sqrt{16\omega_0^2\cos^2\frac{q}{4}-\omega^2}\right] \quad \text{for} \quad k \geqslant \frac{q}{2},\\ \omega_{\frac{q}{4}\pm\frac{k}{2}} &= \frac{1}{2}\left[\omega \pm \cot\frac{q}{4}\sqrt{16\omega_0^2\sin^2\frac{q}{4}-\omega^2}\right] \quad \text{for} \quad k \leqslant \frac{q}{2}.\end{aligned}\tag{A11}$$

For simplicity, we shall consider the case $T = 0$, since the factors containing the Bose-Einstein distribution functions must be carried along with each term and results in quite a cumbersome expression. At $T = 0$, the imaginary part of the two-phonon creation component is given by

$$\mathrm{Im}\,\Pi_q^{(++)}(\omega + i\eta) \propto -\frac{2}{\hbar}\frac{\left|\omega^2 - 4\omega_0^2\sin^2\frac{q}{2}\right|}{16\omega_0^2}\left[\frac{1}{\cos^2\frac{q}{4}\sqrt{16\omega_0^2\cos^2\frac{q}{4}-\omega^2}} + \frac{1}{\sin^2\frac{q}{4}\sqrt{16\omega_0^2\sin^2\frac{q}{4}-\omega^2}}\right]m,\tag{A12}$$

which is composed of the tail of the square root singularity from the upper edge ($k = \pi$) but also has a second square root singularity originating from the extrema at $k = 0$.

The real part of the two-phonon creation component is related to the imaginary part of the component by the Kramer's-Kronig relation. At $T = 0$, the real part can be expressed as an integral that can be reduced to the sum of two elementary integrals

$$\begin{aligned}\mathrm{Re}\,\Pi_q^{(++)}(\omega) &= \frac{1}{2\hbar\omega_0}\int_0^{\pi}\frac{dk}{\pi}\frac{\left|\sin\left(\frac{q}{4}+\frac{k}{2}\right)\sin\left(\frac{q}{4}-\frac{k}{2}\right)\right|}{\left(\frac{\omega}{2\omega_0}\right)-\left|\sin\left(\frac{q}{4}+\frac{k}{2}\right)\right|-\left|\sin\left(\frac{q}{4}-\frac{k}{2}\right)\right|}\\ &= \frac{1}{4\pi\hbar\omega_0}\int_0^{\frac{q}{2}}dk\frac{\cos^2\frac{k}{2}-\cos^2\frac{q}{4}}{\left(\frac{\omega}{4\omega_0}\right)-\cos\frac{k}{2}\sin\frac{q}{4}}+\frac{1}{4\pi\hbar\omega_0}\int_{\frac{q}{2}}^{\pi}dk\frac{\sin^2\frac{k}{2}-\sin^2\frac{q}{4}}{\left(\frac{\omega}{4\omega_0}\right)-\sin\frac{k}{2}\cos\frac{q}{4}}.\end{aligned} \tag{A13}$$

This expression can be further reduced to

$$\begin{aligned}\mathrm{Re}\,\Pi_q^{(++)}(\omega) = &-\frac{1}{\pi\hbar\omega_0}-\frac{\omega}{16\pi\hbar\omega_0^2}\left[\left(\frac{\frac{q}{2}}{\sin^2\frac{q}{4}}\right)+\left(\frac{\pi-\frac{q}{2}}{\cos^2\frac{q}{4}}\right)\right]\\ &+\left(\frac{\omega^2-4\omega_0^2\sin^2\frac{q}{2}}{8\pi\hbar\omega_0^2}\right)\left[\frac{1}{\sin^2\frac{q}{4}}\int_0^{\frac{q}{4}}\frac{\frac{dk}{2}}{\omega-4\omega_0\sin\frac{q}{4}\cos\frac{k}{2}}+\frac{1}{\cos^2\frac{q}{4}}\int_{\frac{q}{4}}^{\frac{\pi}{2}}\frac{\frac{dk}{2}}{\omega-4\omega_0\cos\frac{q}{4}\sin\frac{k}{2}}\right].\end{aligned} \tag{A14}$$

The last two integrals can be evaluated by standard means. The resulting expression for the first integral takes different forms for $\omega > 4\omega_0\cos\frac{q}{4}$ and $\omega < 4\omega_0\cos\frac{q}{4}$. It is evaluated as

$$\begin{aligned}\int_0^{\frac{q}{4}}\frac{dx}{\omega-4\omega_0\sin\frac{q}{2}\cos x} &= \frac{2}{\sqrt{\omega^2-16\omega_0^2\sin^2\frac{q}{4}}}\tan^{-1}\left[\frac{\tan\frac{q}{8}\sqrt{\omega^2-16\omega_0^2\sin^2\frac{q}{4}}}{\omega-4\omega_0\sin\frac{q}{4}}\right] \quad \text{if} \quad \omega^2 > 16\omega_0^2\sin^2\frac{q}{4}\\ &= \frac{1}{\sqrt{16\omega_0^2\sin^2\frac{q}{4}-\omega^2}}\ln\left[\frac{\tan\frac{q}{8}\sqrt{16\omega_0^2\sin^2\frac{q}{4}-\omega^2}+\omega-4\omega_0\sin\frac{q}{4}}{\tan\frac{q}{8}\sqrt{16\omega_0^2\sin^2\frac{q}{4}-\omega^2}-\omega+4\omega_0\sin\frac{q}{4}}\right] \quad \text{if} \quad 16\omega_0^2\sin^2\frac{q}{4} > \omega^2\end{aligned} \tag{A15}$$

and gives rise to a square root singularity above the extrema at $\omega = 4\omega_0\sin\frac{q}{4}$. Likewise, the result for the second integral has different forms for $\omega > 4\omega_0\sin\frac{q}{4}$ and $\omega < 4\omega_0\sin\frac{q}{4}$. It is determined from the indefinite integral

$$\begin{aligned}\int\frac{dx}{\omega-4\omega_0\cos\frac{q}{4}\sin x} &= \frac{2}{\sqrt{\omega^2-16\omega_0^2\cos^2\frac{q}{4}}}\tan^{-1}\left[\frac{\omega\tan\frac{x}{2}-4\omega_0\cos\frac{q}{4}}{\sqrt{\omega^2-16\omega_0^2\cos^2\frac{q}{4}}}\right] \quad \text{if} \quad \omega^2 > 16\omega_0^2\cos^2\frac{q}{4}\\ &= \frac{1}{\sqrt{16\omega_0^2\cos^2\frac{q}{4}-\omega^2}}\ln\left[\frac{\omega\tan\frac{x}{2}-4\omega_0\cos\frac{q}{4}-\sqrt{16\omega_0^2\cos^2\frac{q}{4}-\omega^2}}{\omega\tan\frac{x}{2}-4\omega_0\cos\frac{q}{4}+\sqrt{16\omega_0^2\cos^2\frac{q}{4}-\omega^2}}\right] \quad \text{if} \quad 16\omega_0^2\cos^2\frac{q}{4} > \omega^2,\end{aligned} \tag{A16}$$

which gives rise to a singularity above the upper edge of the two-phonon creation continuum at $\omega = 4\omega_0\cos\frac{q}{4}$, seen in Fig. 17. Due to the singularity in the imaginary part, the real part of the propagator also shows a singularity at the upper edge of the continua. This divergence guarantees that the equation for the bound state of the β lattice, Eq. (23), has a solution above the two-phonon continuum for any positive value of the interaction I_4, no matter how small. The second square root divergence in the imaginary part, due to the states near $k = 0$, is accompanied by a second divergence in the real part. The divergence in the real part guarantees that the equation

$$\sum_{\gamma}\mathrm{Re}\,\Pi_q^{(\gamma)}(\omega) = \frac{1}{I_4} \tag{A17}$$

describing collective modes of the β lattice has a second solution for $4\omega_0\cos\frac{q}{4} > \omega > 4\omega_0\sin\frac{q}{4}$, no matter how weak the interaction I_4 is ($I_4 > 0$). However, since the imaginary part is finite,

$$\sum_{\gamma}\mathrm{Im}\,\Pi_q^{(\gamma)}(\omega) \neq 0, \tag{A18}$$

for this value of ω, one does not find a bound state, but, instead, one finds a resonance located just above the extremum of the two-phonon creation continuum at $\omega = 4\omega_0\sin\frac{q}{4}$. It is noted that the imaginary part of the two-phonon creation component tends to zero smoothly at the lower edge of the continuum since the form factor goes to zero there.

The two-phonon annihilation component and the two-phonon creation component of the propagator are related via

$$\Pi_q^{(++)}(\omega) = \Pi_q^{(--)}(-\omega). \tag{A19}$$

Hence, the real part of $\sum_{\gamma}\Pi_q^{(\gamma)}(\omega)$ is an even function of ω, and the imaginary part $\sum_{\gamma}\Pi_q^{(\gamma)}(\omega+i\eta)$ is an odd function of ω.

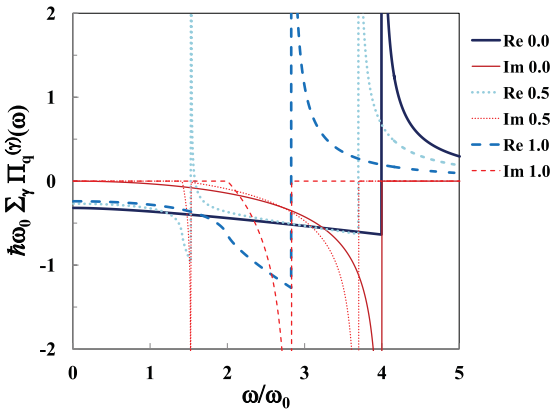

FIG. 17. (Color online) The sum of the real and imaginary parts of the $T = 0$ two-phonon propagators $\sum_\gamma \Pi_q^{(\gamma)}(\omega + i\eta)$ [in units of $(\hbar\omega_0)^{-1}$], for the values of q/π of 0.0, 0.5, and 1.0 (as marked in the legend). The imaginary parts are denoted by the fine red lines and takes on either negative values within the continua or are zero otherwise. The real parts are denoted by the bold blue lines.

At $T = 0$, the component of the two-phonon propagator describing the joint creation-annihilation processes is zero. However, at finite temperatures, the imaginary part is found as

$$\mathrm{Im}\,\Pi_q^{(+-)}(\omega + i\eta) = -\frac{1}{\hbar}\frac{\left|F_{\frac{q}{2}+k}F_{\frac{q}{2}-k}\right|^2}{\left|\frac{\partial}{\partial k}\left(\omega_{\frac{q}{2}+k} - \omega_{\frac{q}{2}-k}\right)\right|}\left[N_{\frac{q}{2}-k} - N_{\frac{q}{2}+k}\right], \quad \text{(A20)}$$

which is to be evaluated at the k values given by the solution of

$$\omega = \omega_{\frac{q}{2}+k} - \omega_{\frac{q}{2}-k}, \quad \text{(A21)}$$

which reduces to the pair of equations

$$\begin{aligned} \omega &= 4\omega_0 \cos\frac{q}{4}\sin\frac{k}{2} \quad \text{for} \quad k \leqslant \frac{q}{2}, \\ \omega &= 4\omega_0 \sin\frac{q}{4}\cos\frac{k}{2} \quad \text{for} \quad k \geqslant \frac{q}{2} \end{aligned} \quad \text{(A22)}$$

At $\omega = 0$, the solutions reduce to $k = 0$ and $k = \pi$, from which it is seen that the Bose-Einstein terms cancel exactly. Hence, the imaginary part vanishes at $\omega = 0$. The imaginary part initially varies linearly with ω. The imaginary part can be evaluated at arbitrary temperatures, but, like the corresponding expression for the two-phonon creation process, it is too cumbersome to display. At sufficiently high temperatures ($k_B T \gg \hbar\omega_0$), the expression simplifies to yield

$$\mathrm{Im}\,\Pi_q^{(+-)}(\omega + i\eta) \propto -2\left(\frac{k_B T\omega}{4\hbar^2\omega_0^2}\right)\left[\frac{1}{\sqrt{16\omega_0^2\cos^2\frac{q}{4} - \omega^2}} + \frac{1}{\sqrt{16\omega_0^2\sin^2\frac{q}{4} - \omega^2}}\right], \quad \text{(A23)}$$

where $0 < \omega \leqslant 2\omega_0 \sin\frac{q}{2}$. As seen in Fig. 18 the difference component of the two-phonon propagator does not introduce any radically new structure to $\sum_\alpha \Pi_q^{(\alpha)}(\omega)$, but only extends the tails of the singularities in the imaginary part of two-phonon creation component to a lower energy range. It is also seen that the effect of increasing temperature is to increase the intensities of the singularities.

APPENDIX B

In this Appendix we present the calculation of the Hamiltonian for the diatomic β lattice.

The harmonic part of the Hamiltonian $\hat{H}_0$ can be written in terms of the Fourier transformed variables and is given by

$$\begin{aligned} \hat{H}_0 = \sum_q \Bigg[&\frac{\hat{P}_{A,q}\hat{P}^\dagger_{A,q}}{2M_A} + \frac{\hat{P}_{B,q}\hat{P}^\dagger_{B,q}}{2M_B}\Bigg] \\ &+ K_2 \sum \Bigg[(\hat{u}_{A,q}\hat{u}^\dagger_{A,q} + \hat{u}_{B,q}\hat{u}^\dagger_{B,q}) \\ &- \cos\frac{q}{2}(\hat{u}_{B,q}\hat{u}^\dagger_{A,q} + \hat{u}_{A,q}\hat{u}^\dagger_{B,q})\Bigg]. \end{aligned} \quad \text{(B1)}$$

This can be diagonalized by two successive canonical transformations. The first canonical transformation is given by

$$\begin{aligned} \hat{P}_{A,q} &= \cos\theta_q \hat{P}_{\alpha,q} + \sin\theta_q \hat{P}_{\beta,q}, \\ \hat{P}_{B,q} &= -\sin\theta_q \hat{P}_{\alpha,q} + \cos\theta_q \hat{P}_{\beta,q}, \\ \hat{u}_{A,q} &= \cos\theta_q \hat{u}_{\alpha,q} + \sin\theta_q \hat{u}_{\beta,q}, \\ \hat{u}_{B,q} &= -\sin\theta_q \hat{u}_{\alpha,q} + \cos\theta_q \hat{u}_{\beta,q}. \end{aligned} \quad \text{(B2)}$$

The Hamiltonian is then written in terms of bosonic creation and annihilation operators

$$\begin{aligned} \hat{P}_{\alpha,q} &= i\sqrt{\frac{\hbar}{2\alpha_q}}(a^\dagger_{\alpha,q} - a_{\alpha,-q}), \quad \hat{u}_{\alpha,q} = \sqrt{\frac{\hbar\alpha_q}{2}}(a^\dagger_{\alpha,q} + a_{\alpha,-q}), \\ \hat{P}_{\beta,q} &= i\sqrt{\frac{\hbar}{2\beta_q}}(a^\dagger_{\beta,q} - a_{\beta,-q}), \quad \hat{u}_{\beta,q} = \sqrt{\frac{\hbar\beta_q}{2}}(a^\dagger_{\beta,q} + a_{\beta,-q}). \end{aligned} \quad \text{(B3)}$$

The values of α_q, β_q, and θ_q are chosen so that the terms that involve the product of two creation operators and terms involving two annihilation operators vanish. This leads to the expressions

$$\begin{aligned} \alpha_q^2 &= \frac{\left(\frac{1}{M_A} + \frac{1}{M_B}\right) + \cos 2\theta_q\left(\frac{1}{M_A} - \frac{1}{M_B}\right)}{4K_2\left(1 + \cos\frac{q}{2}\sin 2\theta_q\right)}, \\ \beta_q^2 &= \frac{\left(\frac{1}{M_A} + \frac{1}{M_B}\right) - \cos 2\theta_q\left(\frac{1}{M_A} - \frac{1}{M_B}\right)}{4K_2\left(1 - \cos\frac{q}{2}\sin 2\theta_q\right)}, \\ \sin 2\theta_q &= \sqrt{\frac{\frac{4}{M_A M_B}\cos^2\frac{q}{2}}{\frac{4}{M_a M_B}\cos^2\frac{q}{2} + \left(\frac{1}{M_A} - \frac{1}{M_B}\right)^2\sin^2\frac{q}{2}}}, \\ \cos 2\theta_q &= -\sqrt{\frac{\left(\frac{1}{M_A} - \frac{1}{M_B}\right)^2\sin^2\frac{q}{2}}{\frac{4}{M_a M_B}\cos^2\frac{q}{2} + \left(\frac{1}{M_A} - \frac{1}{M_B}\right)^2\sin^2\frac{q}{2}}}. \end{aligned} \quad \text{(B4)}$$

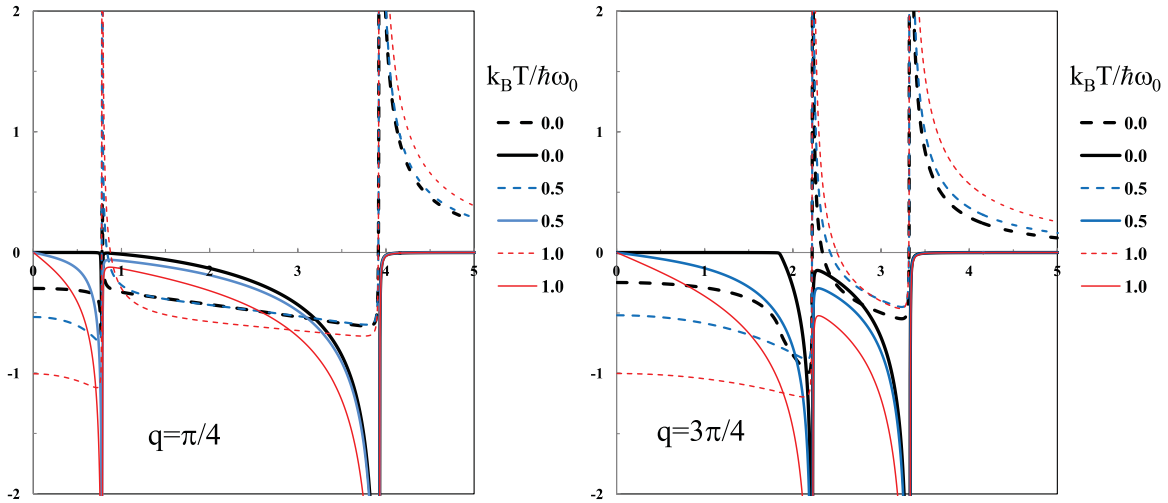

FIG. 18. (Color online) The temperature dependence of the sum of the two-phonon propagators $\sum_\gamma \Pi_q^{(\gamma)}(\omega + i\eta)$ [in units of $(\hbar\omega_0)^{-1}$], for the values of q/π of 0.25 and 0.75, for different values of $(\frac{k_B T}{\hbar\omega_0})$ shown in the legend. The imaginary parts are denoted by the solid lines, and the real parts are denoted by the dashed lines.

The Hamiltonian is then subjected to a second unitary transform

$$\begin{aligned} a^\dagger_{\alpha,q} &= \cos\varphi_q \gamma^\dagger_{1,q} - \sin\varphi_q \gamma^\dagger_{2,q}, \\ a^\dagger_{\beta,q} &= \sin\varphi_q \gamma^\dagger_{1,q} + \cos\varphi_q \gamma^\dagger_{2,q}, \end{aligned} \tag{B5}$$

which diagonalizes the Hamiltonian if φ_q is chosen as

$$\tan 2\varphi_q = \frac{2\sqrt{\alpha_q\beta_q}\cos\frac{q}{2}\cos 2\theta_q}{\beta_q\left(1-\cos\frac{q}{2}\sin 2\theta_q\right) - \alpha_q\left(1+\cos\frac{q}{2}\sin 2\theta_q\right)}. \tag{B6}$$

On substituting the expressions for $\sin 2\varphi_q$ and $\cos 2\varphi_q$, the resulting harmonic Hamiltonian reduces to

$$\begin{aligned} \hat{H}_0 = {} & \frac{\hbar K_2}{2}\sum_q \left\{\alpha_q\left(1+\cos\frac{q}{2}\sin 2\theta_q\right) + \beta_q\left(1-\cos\frac{q}{2}\sin 2\theta_q\right)\right. \\ & \left. - \sqrt{\left[\alpha_q\left(1+\cos\frac{q}{2}\sin 2\theta_q\right) + \beta_q\left(1-\cos\frac{q}{2}\sin 2\theta_q\right)\right]^2 - 4\alpha_q\beta_q\sin^2\frac{q}{2}}\right\}(\gamma^\dagger_{1,q}\gamma_{1,q} + \gamma_{1,q}\gamma^\dagger_{1,q}) \\ & + \frac{\hbar K_2}{2}\sum_q \left\{\alpha_q\left(1+\cos\frac{q}{2}\sin 2\theta_q\right) + \beta_q\left(1-\cos\frac{q}{2}\sin 2\theta_q\right)\right. \\ & \left. + \sqrt{\left[\alpha_q\left(1+\cos\frac{q}{2}\sin 2\theta_q\right) + \beta_q\left(1-\cos\frac{q}{2}\sin 2\theta_q\right)\right]^2 - 4\alpha_q\beta_q\sin^2\frac{q}{2}}\right\}(\gamma^\dagger_{2,q}\gamma_{2,q} + \gamma_{2,q}\gamma^\dagger_{2,q}). \end{aligned} \tag{B7}$$

The above form of the Hamiltonian describes the dispersion relations for the acoustic and optic branches of the phonon excitations. Since direct calculation shows that

$$4\alpha_q\beta_q\sin^2\frac{q}{2} = \frac{1}{K_2}\sqrt{\frac{4}{M_A M_B}}\sin\frac{q}{2} \tag{B8}$$

and

$$\begin{aligned} & \alpha_q\left(1+\cos\frac{q}{2}\sin 2\theta_q\right) + \beta_q\left(1-\cos\frac{q}{2}\sin 2\theta_q\right) \\ & = \sqrt{\frac{1}{2K_2}}\sqrt{\left(\frac{1}{M_A}+\frac{1}{M_B}\right) + \sqrt{\frac{4}{M_A M_B}}\sin\frac{q}{2}}, \end{aligned} \tag{B9}$$

it is seen that the two branches of phonon dispersion relations are given by the conventional expression

$$\begin{aligned} \omega_{i,q} = {} & \sqrt{\frac{K_2}{2}}\left[\sqrt{\left(\frac{1}{M_A}+\frac{1}{M_B}\right) + \sqrt{\frac{4}{M_A M_B}}\sin\frac{q}{2}}\right. \\ & \left. \pm \sqrt{\left(\frac{1}{M_A}+\frac{1}{M_B}\right) - \sqrt{\frac{4}{M_A M_B}}\sin\frac{q}{2}}\right], \end{aligned} \tag{B10}$$

where the optical branch ($i = 1$) corresponds to the positive sign and the acoustic branch ($i = 2$) corresponds to the negative sign. In the above derivation it has been implicitly assumed that $\sin\frac{q}{2}$ has a positive value.

The anharmonic interaction $\hat{H}_{\rm int}$ can be written in the form of a sum of two separable momentum-conserving interactions

$$\hat{H}_{\rm int} = \left(\frac{K_4}{12N}\right) \sum_{k_1,k_2,k_3,k_4} \Delta_{k_1+k_2+k_3+k_4} \prod_{j=1}^{4} \{\exp[-ik_j/4]\hat{u}_{A,k_j} - \exp[+ik_j/4]\hat{u}_{B,k_j}\} + \left(\frac{K_4}{12N}\right) \sum_{k_1,k_2,k_3,k_4} \Delta_{k_1+k_2+k_3+k_4} \times \prod_{j=1}^{4} \{\exp[+ik_j/4]\hat{u}_{A,k_j} - \exp[-ik_j/4]\hat{u}_{B,k_j}\}. \tag{B11}$$

For a set of fixed k_j values, the pairs of interaction operators are mutually Hermitean conjugate. The interaction can be put into the second quantized form

$$\hat{H}_{\rm int} = \left(\frac{K_4\hbar^2}{48N}\right) \sum_{m=1}^{2} \left[\sum_{k_1,k_2,k_3,k_4} \Delta_{k_1+k_2+k_3+k_4} \prod_{j=1}^{4} \times \left\{ \sum_{i=1}^{2} F_{i,k_j}^{(m)} \left(\gamma_{i,k_j}^{\dagger} + \gamma_{i,-k_j}\right) \right\} \right], \tag{B12}$$

where the form factors for each separable interaction $F_{i,k}^{(m)}$ are complex numbers. For the first separable interaction ($m = 1$), the form factors are given by

$$\begin{aligned} F_{1,k}^{(1)} = \cos\frac{k}{4}[&\alpha_k \cos\varphi_k(\cos\theta_k + \sin\theta_k) \\ &+ \beta_k \sin\varphi_k(\sin\theta_k - \cos\theta_k)] \\ &- i \sin\frac{k}{4}[\alpha_k \cos\varphi_k(\cos\theta_k - \sin\theta_k) \\ &+ \beta_k \sin\varphi_k(\sin\theta_k + \cos\theta_k)] \end{aligned} \tag{B13}$$

and

$$\begin{aligned} F_{2,k}^{(1)} = \cos\frac{k}{4}[&-\alpha_k \sin\varphi_k(\cos\theta_k + \sin\theta_k) \\ &+ \beta_k \cos\varphi_k(\sin\theta_k - \cos\theta_k)] \\ &-i \sin\frac{k}{4}[-\alpha_k \sin\varphi_k(\cos\theta_k - \sin\theta_k) \\ &+ \beta_k \cos\varphi_k(\sin\theta_k + \cos\theta_k)]. \end{aligned} \tag{B14}$$

For the second separable interaction ($m = 2$), the form factors $F_{i,k}^{(2)}$ are given as the complex conjugates of the $F_{i,k}^{(1)}$:

$$F_{i,k}^{(2)} = \left(F_{i,k}^{(1)}\right)^*. \tag{B15}$$

[1] J. Scott-Russell, Fourteenth Meeting of the British Association for the Advancement of Science, 1844.
[2] D. J. Korteweg and G. de Vries, Phil. Mag. Ser. 5 **39**, 422 (1895).
[3] P. S. Riseborough, Phil. Mag. **91**, 997 (2011).
[4] N. J. Zabusky and M. D. Kruskal, Phys. Rev. Lett. **15**, 240 (1965).
[5] C. S. Gardner, C. S. Greene, M. D. Kruskal, and R. M. Miura, Phys. Rev. Lett. **19**, 1095 (1967).
[6] P. D. Lax, Commun. Pure Appl. Math. **21**, 467 (1968).
[7] M. Toda and M. Wadati, J. Phys. Soc. Jpn. **34**, 18 (1973).
[8] A. Seeger, H. Donth, and A. Kochendorfer, Z. Phys. **134**, 173 (1953).
[9] H. J. Mikeska, J. Phys. C **11**, L29 (1978).
[10] K. M. Leung, D. W. Hone, D. L. Mills, P. S. Riseborough, and S. E. Trullinger, Phys. Rev. B **21**, 4017 (1980).
[11] P. S. Riseborough and S. E. Trullinger, Phys. Rev. B **22**, 4389 (1980).
[12] P. S. Riseborough, D. L. Mills, and S. E. Trullinger, J. Phys. C **14**, 1109 (1980).
[13] A. J. Sievers and S. Takeno, Phys. Rev. Lett. **61**, 970 (1988).
[14] R. S. MacKay and S. Aubry, Nonlinearity **7**, 1623 (1994).
[15] R. F. Dashen, B. Hasslacher, and A. Neveu, Phys. Rev. D **10**, 4114 (1974); **11**, 3424 (1975).
[16] L. S. Schulman, Phys. Rev. A **68**, 052109 (2003); Phys. Status Solidi B **237**, 124 (2003).
[17] E. K. Skylanin, L. A. Takhtadzhyan, and L. D. Faddeev, Theor. Math. Phys. **40**, 688 (1979).
[18] L. D. Faddeev and V. E. Korepin, Phys. Rep. **42**, 1 (1978).
[19] K. Maki and H. Takayama, Phys. Rev. B **22**, 5302 (1980).
[20] P. S. Riseborough and P. Kumar, J. Phys. Condens. Matter **1**, 7439 (1989).
[21] Q. Xia and P. S. Riseborough, J. Phys. (Paris) **49**, 1587 (1988).
[22] S. Aubry, Physica D **103**, 201 (1997).
[23] S. Flach and C. R. Willis, Phys. Rep. **295**, 181 (1998).
[24] S. Flach and A. V. Gorbach, Phys. Rep. **467**, 1 (2008).
[25] R. A. Pinto and S. Flach, in *Dynamical Tunneling: Theory and Experiment*, edited by S. Keshavamurthy and P. Schlagheck (Taylor and Francis, Abingdon, 2011), pp. 339–382.
[26] A. C. Scott, J. C. Eilbeck, and H. Gilhoj, Physica D **78**, 194 (1994).
[27] W. Z. Wang, J. T. Gammel, A. R. Bishop, and M. I. Salkola, Phys. Rev. Lett. **76**, 3598 (1996).
[28] L. Proville, Phys. Rev. B **71**, 104306 (2005).
[29] L. S. Schulman, D. Tolkunov, and E. Mihokova, Phys. Rev. Lett. **96**, 065501 (2006).
[30] E. Fermi, J. Pasta, and S. Ulam, Los Alamos National Laboratory, unpublished report, Document LA-1940 (May 1955).
[31] S. Flach and A. V. Gorbach, Chaos **15**, 015112 (2005).
[32] Z. Ivic and G. P. Tsironis, Physica D **216**, 200 (2006).
[33] Hu Xin-Guang and Tang Yi, Chinese Phys. B **17**, 4268 (2008).
[34] G. P. Berman and N. Tarkhanov, Int. J. Theor. Phys. **45**, 1885 (2006).
[35] J. C. Eilbeck, H. Gilhoj, and A. C. Scott, Phys. Lett. A **172**, 229 (1993).
[36] M. E. Manley, A. J. Sievers, J. W. Lynn, S. A. Kiselev, N. I. Agladze, Y. Chen, A. Llobet, and A. Alatas, Phys. Rev. B **79**, 134304 (2009).
[37] A. A. Maradudin and A. E. Fein, Phys. Rev. **128**, 2589 (1962).
[38] R. A. Cowley, Adv. Phys. **12**, 421 (1963).
[39] S. W. Lovesey, *Theory of Neutron Scattering from Condensed Matter* (Oxford University Press, Oxford, 1984).

[40] S. Basu and P. S. Riseborough, [http://dx.doi.org/10.1080/14786435.2011.607141].
[41] L. Proville, Physica D **216**, 191 (2006).
[42] P. L. Leath and B. P. Watson, Phys. Rev. B **3**, 4404 (1971).
[43] R. Livi, M. Spicci, and R. S. MacKay, Nonlinearity **10**, 1421 (1997).
[44] P. Maniadis, A. V. Zolotaryuk, and G. P. Tsironis, Phys. Rev. E **67**, 046612 (2003).
[45] G. James and P. Noble, Physica D **196**, 124 (2004).
[46] K. Yoshimura, Nonlinearity **24**, 293 (2011).
[47] P. S. Riseborough, Solid State Commun. **48**, 901 (1983).
[48] N. Levinson, Mat.-Fys. Medd. **25**, 1 (1949).
[49] A. A. Maradudin and P. A. Flinn, Phys. Rev. **129**, 2529 (1963).
[50] J. N. Texeira Rabelo, E. S. Cardoso, and V. I. Zubov, Mod. Phys. Lett. B **14**, 1001 (2000).
[51] V. Fleurov, Chaos **13**, 676 (2003).
[52] P. S. Riseborough and G. F. Reiter, Phys. Rev. B **27**, 1844 (1983).